Chapter1 - Introduction to the project

1.1 Statement of Problem

Advances in analytical techniques and computational speed have made the investigation of increasingly complex structural behavior possible. Previously, compromising simplifications have been required to analyze nonlinear dynamic behavior of structures, especially when modeling complex new structural devices. While these simplifications are useful, research shows that simplifications can lead to decreasing accuracy for increasingly complex structural models. The type of nonlinear behavior exhibited by the structure, the behavior of any seismic protection devices, and the inclusion of multiple degrees of freedom add to the complexity of a structure from an analytical standpoint. To gain a complete picture of the dynamic behavior of structures, investigation of complex systems with seismic protection devices is necessary for accurately evaluating nonlinear dynamic structural behavior.

As degrees of freedom are added to a structure, the analytical complexity grows. Single degree of freedom (SDOF) models present a simplified view of the various aspects of nonlinear dynamic structural behavior, and are used to obtain a generalized idea of structural behavior. The investigation of multiple degree of freedom (MDOF) systems results in increased complexity and accuracy in predicting structural behavior.

Due to its highly sensitive nature, structural behavior of particular concern for structural analysis is dynamic instability. Analytical accuracy becomes crucial, especially for the evaluation of how stability may be controlled. The accuracy of structural analysis is at stake when making choices regarding the complexity of the analysis chosen for structures that exhibit instability. Advanced modeling and analysis techniques are required to obtain the most accurate results for the nonlinear dynamic behavior of structures. Structural engineering methods focus on eliminating the unpredictable nature of nonlinear dynamic structural behavior.

Many types of seismic protective devices are available for increased structural stability and dissipation of dynamic energy. These devices include dampers, base isolators, and braces. Each device type instills explicit an behavioral characteristic into a structure with the goal of controlling specific dynamic parameters. The stabilizing

potential of elastic nonlinear devices known as hyperelastic braces are of particular interest with regard to MDOF structures near collapse. The theoretical function of these braces is to add increasing stiffness to a structure as deformation increases to prevent instability at high levels of acquired displacement. Increased stiffness at low levels of displacement is not desired due to the increase of system forces that would occur for service-level loads. Hyperelastic braces behave elastically along a nonlinear stress-strain relationship defined by a cubic polynomial, and may be analytically implemented through the use of a hyperelastic material in a diagonal brace.

1.2 Objective of Project

The objective of the proposed research is to investigate the stabilizing effects of hyperelastic devices on multiple degree of freedom systems that exhibit signs of instability under extreme seismic loading. To evaluate the influence of the new devices on specific behavioral parameters and response measures, the models of structures containing hyperelastic devices will be investigated under varying levels of ground motion using incremental dynamic analysis (IDA). Specifically, the influence of hyperelastic braces on base shear and interstory drift will be investigated as the main parameters of interest.

Hyperelastic braces differ from other nonlinear devices in that they do not dissipate energy and they are designed to only influence structural behavior nearing instability. Specific hyperelastic relationships may be formed to suit a particular system based on yield strength, stiffness, and ductility demand. This type of behavior is beneficial for structural engineering due to the ability to avoid increased system forces at low levels of dynamic excitation and to increase structural predictability. Hyperelastic braces may be beneficial to any structure that experiences nonlinear dynamic behavior, not just unstable systems.

The increase in structural stability from hyperelastic devices may be expected to reduce the amount of dispersion observed in the IDA results. Dispersion occurs due to systemic influences like residual displacement and yield sequence, as well as due to analytical influences such as ground motion characteristics. Based on the variance of the

data contained in the IDA curves, hyperelastic braces will be analyzed for their influence on the systemic sources of dispersion.

From the analyses performed on the MDOF structures, the most effective brace materials may be identified and evaluated for future applications. Also, a quantitative measure of the brace effectiveness is desirable for comparison with other devices. The influences of hyperelastic braces on the structural stability will be identified using the IDA curves created for each model and each ground motion. The stabilizing effects of the braces will be compared to the related increases in base shear to gain an overall view of the efficiency of hyperelastic bracing. These measures of the influence of hyperelastic braces will increase the understanding of how the new devices may be used for structural engineering.

1.3 Scope of Project

To determine the effectiveness of hyperelastic braces on nonlinear dynamic behavior of structures, a series of analyses will be performed on a planar MDOF structure. The investigation will focus on one MDOF model with bilinear yielding properties. The behavior of the structure will be evaluated on the basis of maximum interstory drift and maximum base shear for the structure. The models will be compared to the behavior of the structure without braces to determine how the new device influences the behavior of the structure.

To evaluate such complex structural behavior, two analysis software packages will be applied to the proposed models. The primary software package is known as the Open System for Earthquake Engineering Simulation, or OpenSees (PEER, 1999). The capabilities of this program have been adapted for use with the proposed type of structural modeling, and have proven to be capable of obtaining the desired results. Also, the analysis program Drain-2DX (1993) will be used to analyze similar models to provide a cross check for the new software package and to validate the behavior of the baseline MDOF model before hyperelastic braces are included. The two programs offer distinct and separate advantages in analyzing the complexities involved with nonlinear dynamic analysis of structures, and thus should provide abundant insight for the proposed models.

1.4 Overview of Thesis

An overview of this paper may be helpful in understanding the chosen course for the research and how the modeling will progress for the proposed set of analyses. Each chapter investigates a new aspect of the research pertaining to the overall goal of assessing the effectiveness of hyperelastic braces.

An analogous view for the layout of this document is comparable to assembling a simple building, to keep things in terms of structural engineering. The first three chapters lay out the relevant background information for these analyses, and represent the foundation of the analogous building. Chapter 1 establishes the purpose and importance of the proposed research, and sets forth the guidelines for the breadth of detail that the analyses will cover. Chapter 2 provides background information relevant to nonlinear dynamic analysis and behavior of structures. Modeling techniques and analysis issues are investigated that are relevant to the behavior of instable structures. Chapter 3 provides an overview of hyperelastic behavior as it pertains to the devices that will be investigated with the MDOF structural systems. These three chapters round out the foundation of the research and provide a sufficient base to support the following analyses.

The next stage in the analogous structure is the structural members themselves: the walls, floors, and ceilings. This is comparable to Chapters 4 and 5 where the actual structural investigation is performed. Chapter 4 presents the details surrounding the models investigated. All of the system properties are given in this chapter, as well as their importance on the overall behavior of the system. This is particularly important since the proposed investigation focuses on such a specific area of structural behavior as instability and collapse. Chapter 5 presents the findings and results of the model sets discussed in Chapter 4. All of the important behavioral influences related to the hyperelastic devices are discussed in this chapter, along with the supporting data and any issues noticed with the correlation between the two programs used.

The final stage of building this simple structure is providing a roof, or an adequate finish to the structure beneath it. Chapter 6 presents the conclusions and recommendations that can be formed based on the results from the models given in Chapters 4 and 5. The overall conclusions regarding how hyperelastic devices influence MDOF structures that become unstable under dynamic loading are drawn out and justified based on the

supporting data. Also, recommendations regarding application of hyperelastic devices to real structures are presented along with the conclusions. The recommendations include the creation of practical devices that exhibit hyperelastic behavior as well as suggestions for future investigation for hyperelastic devices.

Chapter 2 - Background Research on Nonlinear Dynamic Analysis and Behavior

2.1 Incremental Dynamic Analysis

Incremental dynamic analysis (IDA) involves subjecting a structure to one or more ground motions scaled to several levels of intensity (IM) and recording the structural response through damage measures (DM). The results are then plotted (scaled acceleration vs. DM) to construct an IDA curve, and the various limit states for structural behavior can be identified. IDA involves a series of nonlinear dynamic analyses performed under sequentially scaled versions of an accelerogram (Vamvatsikos and Cornell, 2002).

To discuss the theory and application of incremental dynamic analysis, establishing background information is important. From a single IDA curve, many properties and limit states of structural performance may be identified, specifically for nonlinear dynamic structural behavior. Hardening and softening structural stiffness, yield points, and overall system performance can be identified from the shape characteristics of IDA curves. Limit states and structural capacities may be based on intensity measures (y axis) or damage measures (x axis) of the IDA curve.

The behavior of a structure cannot be fully captured by a single IDA curve; therefore it is more informative to look at a range of curves generated under multiple scaled records. Differences between the results for a single structure obtained from multiple similar-type ground motions is called dispersion. Dispersion is a source of uncertainty and thus detracts from the deterministic approaches for analyzing dynamic structural behavior

Dispersion is best described as randomness in structural behavior between records. The use of probabilistic characterization has been instituted to account for this variability in structural behavior. The application of probabilistic characterization leads to the use of performance based earthquake engineering frameworks, where the concern is with “the estimation of the annual likelihood of the event that the demand exceeds the limit state or capacity” (Vamvatsikos and Cornell, 2002). Associations can be made to relate the IDA method to the yield reduction R-factor, and graphical similarities are found

between IDA and the nonlinear static pushover method. Solution algorithms for using IDA in a computer analysis program are easily formed and implemented for computational efficiency.

Incremental dynamic analysis techniques are applicable to the proposed modeling of structures with hyperelastic braces because they provide the most comprehensive and informative picture of nonlinear structural behavior. Thus, a wide range of influence of hyperelastic braces on structural behavior may be evaluated with IDA

2.2 Analysis Considerations for IDA

IDA curves can be generated for a multitude of ground motion scenarios, and a wide range of behavioral data may be accumulated for any single structure. Therefore, summarizing the behavioral data in a statistical format is necessary to measure the amount of randomness introduced by the selected earthquake records (Vamvatsikos and Cornell, 2002). The damage measure (DM) values for all of the IDA curves may be summarized into their 16th, 50th, and 84th percentiles for statistical analysis of the spread of the data. Dispersion is defined as the coefficient of variation between the data sets formed under IDA. The results of these summaries may be applied to performance based earthquake engineering (PBEE) through the estimation of the mean annual frequency (MAF) of exceeding a specific level of structural demand.

Commercially available software provides a practical approach for performing IDA and interpreting the results for a variety of structural considerations. Considerations may involve an array of material behaviors and dynamic behavioral parameters for any number of degrees of freedom in a structure.

Several steps may be defined for performing IDA. First, the appropriate ground motions and damage measures must be chosen for a structural system. Next, the ground motion records must be appropriately scaled. After the analysis is performed, the IDA curves must be properly interpolated so that the data sets can be summarized.

Important issues exist regarding the selection of analysis techniques and the subsequent influence on IDA results. These choices include selection of a numerical convergence method for curve generation, tracing algorithm, interpolation method, and limit state definitions. When increasingly complex behaviors are investigated, the

sensitivity of a structure to these choices of techniques increases greatly. The important part of each analysis option involved in IDA is to understand how each choice influences the analysis and how informative the IDA data can be for portraying nonlinear dynamic behavior.

A comparison of the nonlinear static pushover curve (SPO) versus the median IDA curve shows similarities in structural behavior between curve segments. The median IDA curve is defined by the 50^{th} percentile resulting from a range of IDA curves performed on a structure. Similarities are found through investigation of numerous SDOF systems under IDA and comparison of the results to the related SPO curve. Behavior as complex as a quadrilinear backbone may be used for the SPO curves which can be related to a specific IDA curve. Generally, the worst SPO case results in the most accurate IDA results. The results of these comparisons show that a reasonable level of accuracy in results may be obtained from information contained in the SPO analysis as a full IDA procedure. Reliable results may be found at a fraction of the computation time by using these relationships between IDA and SPO (Vamvatsikos and Cornell, 2002).

The above method shows that relationships between static and dynamic analyses do exist, and that fully understanding the behavior of complex systems begins with knowledge gained through simple analytical techniques. The progression of analysis techniques has been developed using relationships based on fundamental structural behavior, thus the optimization of advanced methods for nonlinear dynamic analysis is dependent on the underlying behavioral theories.

2.3 IDA versus Other Analysis Methods

Important theoretical observations may be made by comparing IDA to other related analysis types, such as probabilistic framework methods and design based methods. The goal of these methods is to create probabilistic seismic demand models (PSDM) for evaluation of the range of possible dynamic behavior. The demand-based methods attempt to represent a structure's range of seismic behavior based on probabilities, or the "probability of exceeding specified structural demand levels in a given seismic hazard environment" (Mackie and Stojadinovic, 2002). The design-based methods seek to determine the maximum allowable response and design the building

accordingly. New structural devices seek to limit the need for these other methods by limiting the range of dynamic behavior, and thus increasing the predictability

Probabilistic seismic demand analysis (PSDA) forms a demand model using an analysis technique composed of many ground motions grouped into bins to represent a range of seismic intensities. The IDA approach uses a few select ground motions applied over the structure, each of which are incrementally scaled to represent a range of seismic intensities. The only variance in the formulation of the probabilistic demand models is the chosen method of analysis, with the differences mentioned previously (bin approach vs. scaling). Based on a comparison of the two analysis types, both can be used interchangeably to create PSDMs for performance-based analysis. Similar computational effort produces results with similar confidence levels for the median values as long as an adequate number of ground motions are considered (Mackie and Stojadinovic, 2002). The newly proposed research seeks to increase structural performance predictability, and thus increase the confidence levels at which the demand models may be created.

2.4 Seismic Risk - Applying IDA

Performance-based analysis of structures is specifically concerned with the susceptibility of a structure to direct damage from a seismic event. Thus, the use of advanced analytical techniques is beneficial to the accuracy of damage prediction. Structural performance is evaluated by the calculation of the annual probability of exceeding a certain level of nonlinear damage due to a seismic event. Conventional seismic hazard analysis (SHA) is primarily based on observations made with linear SDOF systems. Previously, these SHA procedures have been modified to estimate the direct seismic risk of post elastic damage in MDOF systems. Currently, probabilities are being constructed for more complex structures through the use of analysis techniques like IDA. IDA increases the accuracy of the hazard analysis and narrows the range of possible structural behavior. This makes the application of specific device behaviors more accurate and in-tune with the predicted behavior of a structure

For assessing seismic risk in an analysis context, spectral acceleration (S_a) and ground motion duration (T_D) are traditionally the primary variables of interest for the

damaging potential of an earthquake event. Studies have found no direct dependence between T_D and the damage induced on a structure (Bazzurro and Cornell, 1994a).

To characterize the damage potential of a seismic event, nonlinear response-based factors are used to associate a linear SDOF system with real MDOF systems. The nonlinear response factors account for ground motion parameters as well as nonlinear structural parameters. For MDOF systems, this factor may vary according to location of damage in the structure, type of damage, and the level of damage experienced. Nonlinear response factors are shown to have no dependence on magnitude (M) or distance (R) of a given seismic record, and are proven to meet the statistical criteria (median and coefficient of variation) for probabilistic analysis of the seismic risk for nonlinear damage in MDOF systems (Bazzurro and Cornell, 1994a).

However, the use of nonlinear response factors is made unnecessary by the increasing computing power and analysis accuracy available on modern computers. With these advances, full scale models may be analyzed at a fraction of the computational cost and with greater accuracy than previously available. This computational advantage eliminates the need for simplifications such as nonlinear response factors for predicting nonlinear behavior in MDOF systems.

Based on the methodology by Bazzurro and Cornell for seismic hazard analysis for post-elastic damage in nonlinear MDOF structures, realistic 3-dimensional structures have been analyzed for their response. This represents a significant step forward in analytical accuracy. Structures may display a variety of nonlinearities including material, soil, geometric, and local (buckling) and global (P-Δ) effects. When applied to 3-dimensional nonlinear structures, the methodologies allow the determination of seismic risk curves for global and local damage measures considered to be critical for these structures. The methodology proves to be applicable to realistic cases for determining seismic risk for complex structures based on simpler structures (Bazzurro and Cornell, 1994b).

Overall, seismic risk analysis seeks to establish the probability that a structure will acquire a specific level of damage due to a specified seismic event. New analytical techniques like IDA, when coupled with increased computational power, increase the accuracy of this prediction. As these methods become more fine-tuned, the effect of

seismic protective devices may be directly evaluated for the amount of influence they may have on mitigating structural seismic risk.

2.5 Damage Measures – Quantifying Nonlinear Behavior

An extensive body of work exists on characterizing seismic damage in structures. Ductility demand is one of the most commonly considered damage measures, relating damage to the maximum allowable deformation. Two goals arise out of the use of damage indices: prediction of the structural damage and post-earthquake evaluation of sustained damage (Sorace, 1998). In order to improve the accuracy of damage prediction, the damage induced by seismic loadings can be estimated. The damage estimates are based on the principles of various damage indices in order to reduce the variation introduced by free coefficients. The free coefficients are mathematical variables present in the expressions for each damage index, and comparative analysis between the indices provides a means of calibration through statistical-numerical investigation.

While there are numerous damage measures for the nonlinear behavior of structures, the various methods may be calibrated against each other through the free coefficients found in the mathematical formulation of each. Multiple damage measures are required to get an adequate picture of seismic response, and to verify the calibration of each response measure.

Three independent methodologies have been proposed by Cornell, Wen, and FEMA 273 for predicting maximum nonlinear responses due to seismic excitation. Although the three methods have been developed with separate objectives, they may be brought under the same perspective for comparison and increased accuracy. The goal of such a comparison is to increase the accuracy of predicting structural seismic response through verification of results obtained from independent methods (Bazzurro et.al., 1998)

The FEMA method relies on a simplified procedure where the deformations (global and local) are predicted through the use of period-dependent modification factors (C_1, C_2, and C_3). This method is formed from pushover analyses that are used to predict target displacements. The target displacements are then related to the deformation demands of specific components in a structure.

The method proposed by Wen estimates the probabilities of exceeding limit states for a MDOF structure. The dependence of the structural response to magnitude (M) and distance (R) is combined into a correlation factor (C), which is applied as a type of scale factor to the ground motions. The Monte Carlo method is then used to evaluate the factors and generate a synthetic record to represent all possible past and future events for a structure.

The Cornell method attempts to estimate the annual probability of exceeding a certain measure of nonlinear response. The response is dependent on spectral acceleration, fundamental frequency, and damping level present in the structure, and the location/building characteristics are constant.

The three methods can be compared and contrasted with respect to their assumptions, their efficiency, and their potential application (Bazzurro and Cornell, 1998). All of the options for measuring structural response are valid based on their original intent and application, therefore choosing the most appropriate damage measure depends on project relevancy.

Three more response measures have been evaluated for the calibration of the free coefficients in past research (Sorace, 1998). The Park-Ang model is based on a linear combination of deformation damage and cumulative plastic strain energy. The McCabe-Hall model uses the hysteretic energy as the damage measurement, using a power function of the global dissipated plastic energy. The plastic fatigue index is based on an analogy between seismic response and low-cycle fatigue behavior of materials under cyclic loading. The free coefficients formed by comparing the three different response measures among each other were shown to exhibit small scatter, and the final damage indices were stable with respect to their respective mechanical parameters (hysteretical loading-unloading schemes, cyclic failure conditions, and index expressions). Also, the index values calculated were successfully correlated to post testing values. Results are expected to be more scattered for complex structural systems, which suggests the adoption of more refined statistical computational techniques (Sorace, 1998).

Although these methods strive for higher levels of accuracy in establishing structural damage levels, IDA is the next step in the application of techniques for calibration of damage measure. For damage index calibration, the use of IDA curves can allow for statistical comparison over a range of seismic demand for a single damage

index. Each damage measure may then be compared and calibrated to increase the damage prediction accuracy. With increases in computing and programming power, IDA can account for a variety of nonlinearities without sacrificing accuracy due to structural complexity. Modifying the conventional SHA procedures based on simpler structures to account for higher levels of complexity is no longer necessary. IDA can make use of the summarization techniques developed for these methods and produce a more reliable and accurate model of annual probabilities of exceeding specific damage levels during a seismic event.

2.6 Dispersion and Uncertainty in Dynamic Results

The deterministic advantages of incremental dynamic analysis may be maintained through efforts to reduce the amount of dispersion present in the results. Sources of dispersion come from either analytical discrepancies or from systemic influences. Refined analytical techniques along with better computational methods help refine numerical issues with such complex analyses. Systemic causes of dispersion may include P-Delta effects and yield sequence within a structure. To account for the systemic causes of dispersion, the addition of structural devices may help reduce the variability in structural behavior. Accounting for both systemic and analytical sources of dispersion will reduce sources of error that contribute uncertainty to the results IDA

Seismic events, residual displacements, and member yielding are all factors which can contribute to dispersion in the results of incremental dynamic analysis of structures. Singly, each one of these factors is proven to increase the amount of variability in the analysis results on structures. Combined, each factor compounds the variability in the analysis results, and determining the most effective and accurate way of accounting for each factor is important in improving the reliability of IDA. Due to the behavioral variances in the results found through incremental dynamic analysis, a probabilistic format is used to quantify the amount of variability in the results instilled either naturally or through the listed factors (Vamvatsikos and Cornell, 2002).

The investigation of nonlinear fluid viscous dampers (Oesterle, 2002) proves that residual displacements are a source of IDA dispersion. Residual displacements are a permanent deformation instilled in a structural system by a ground motion through

member yielding. Residual displacements will affect the structural behavior in terms of the reaction of the structure to any further seismic loading. If a residual displacement is instilled into a structure, when it occurs and how it influences further behavior of the structure under a seismic event are dependent on the record variance and structural response frequency. Record variance refers to the amount of variability in peak acceleration values and frequency content in ground motion record. Therefore, dual variability may be introduced into the behavior of the structure in the form of event randomness and varying structural response frequency.

In the analyses performed on the nonlinear fluid viscous dampers (Oesterle, 2002), the conclusions are made by quantifying the residual displacement for a 9 story building located in Los Angeles and taking running averages. The results show that using a hardening damper with a damping exponent (α) equal to 1.5 is the most effective in reducing residual displacements. The damping exponent defines the rate of increase for the force-velocity relationship in a damping device. This damper type was compared for its effectiveness versus linear (α=1.0) and softening (α=0.75) dampers. By investigating the related IDA curves for these damper types, the results show consistently less dispersion with decreased residual displacements for the hardening damper.

Some dispersion in IDA results may come from the randomness of the earthquake events. Differences between records include varying sequences of peak accelerations, varying magnitudes, varying rate of peak occurrence (peak frequency), and varying time of peak occurrence. The combination of these factors forms a general measure of the intensity randomness within a given earthquake record (Oesterle, 2002). A Fast Fourier Transform (FFT) frequency plot can be used to compare magnitude and frequency of the harmonics present in different ground motion records. By subjecting a structure to a series of events which are random by nature, the small variances in the record characteristics may influence the results in a significant way. The chaotic nature of the structural response occurs due to the sensitivity of a structure once it reaches the nonlinear portion of its material behavior.

Due to the stabilizing effects of hyperelastic braces, the amount of dispersion observed in the IDA results is expected to decrease. Hyperelastic braces are similar in nature to the hardening devices investigated by Oesterle (2002). However, the braces provide only an elastic stiffening response while the dampers are used to dissipate an

increasing amount of energy. Both devices provide an increasing amount of response as a structure gains deformation. The proposed research seeks to investigate the stabilizing effects of hyperelastic braces in structures, and the influence of the braces on dispersion.

2.7 Sensitivity of Dynamic Structural Response

The static pushover curve gives insight into the sensitivity of a structure to yielding. When analyzed on an event-to-event basis, the yield points are commonly seen to occur within a thin zone of applied lateral force when member strengths are similar. This means that as lateral loads (i.e., seismic events) are applied to a structure to the point of yield, the building members tend to yield at very nearly the same strength value as other members in the same structure. This results in a high sensitivity of structural behavior to the yielding sequence.

Yielding in a structure will also affect the reaction frequency. This is confirmed in a study conducted on seismic performance and reliability of structures using incremental dynamic analysis (Vamvatsikos and Cornell, 2002). The reaction frequency of a structure is the frequency at which the structure responds to periodic excitation. As a structure undergoes the first stages of yielding, the original response frequency changes from lower to higher modes. Higher modes become more dominant as yielding occurs in a structure due to the associated loss of strength. The loss of strength causes the dominant period of vibration to increase due to the influence of the higher mode reaction frequencies of a structure. A structure which is initially dependent only on the first mode frequency will likely become dependent on higher modes after yielding occurs in the structure.

This behavior highlights the sensitivity of structural behavior as yielding occurs. More dispersion will occur in the IDA results of a highly sensitive structure. The implementation of seismic protective devices can help prevent such sensitivity to dynamic excitation and lead to greater predictability in structural behavior.

Since structural behavior and reaction frequency affect IDA accuracy, the sensitivity of the results to the yielding sequence within a structure is worth investigating. One approach for analyzing the effect on IDA dispersion and variability is to run IDA analyses in which the structure has an imposed and controlled sequence of member

yielding. This control could be made possible by using limited strength hinges at the beam-column joints for a structure and running a comparative series of incremental dynamic analyses.

While structures may be designed to sustain a certain level of inelastic deformation in order to dissipate seismic energy, concerns exist in the amount and specification of inelastic deformation allowed within a structure. Methods such as Response History Analysis, Random Vibration Analysis, and Linear Elastic Response Spectra are available for constructing an inelastic design response spectrum (IDRS). From these methods, criteria may be established for the amount of inelastic displacement a particular structure can realistically absorb before dynamic instability becomes a risk. However, the amount of dispersion and variability in the methods shows that they cannot be viewed as reliably limiting maximum ductility demands to specified values (Mahin and Bertero, 1981).

2.8 Initial Study of Hyperelastic Behavior

Prior to the study described for the present research, a pilot study of the effect of hyperelastic devices on SDOF systems was performed by Changsun Jin (Jin, 2003). Hyperelastic braces have been studied as a means of increasing structural reliability. Hyperelastic materials behave elastically along a nonlinear stress-strain relationship defined here by a cubic polynomial. The primary concept with hyperelastic braces is to add increasing stiffness as deformation increases to prevent dynamic instability. This material property is defined by a polynomial curve that is concave upwards, indicating that the material gains stiffness as it deforms. The graph of an arbitrary hyperelastic stress-strain relationship is shown in Figure 2.1

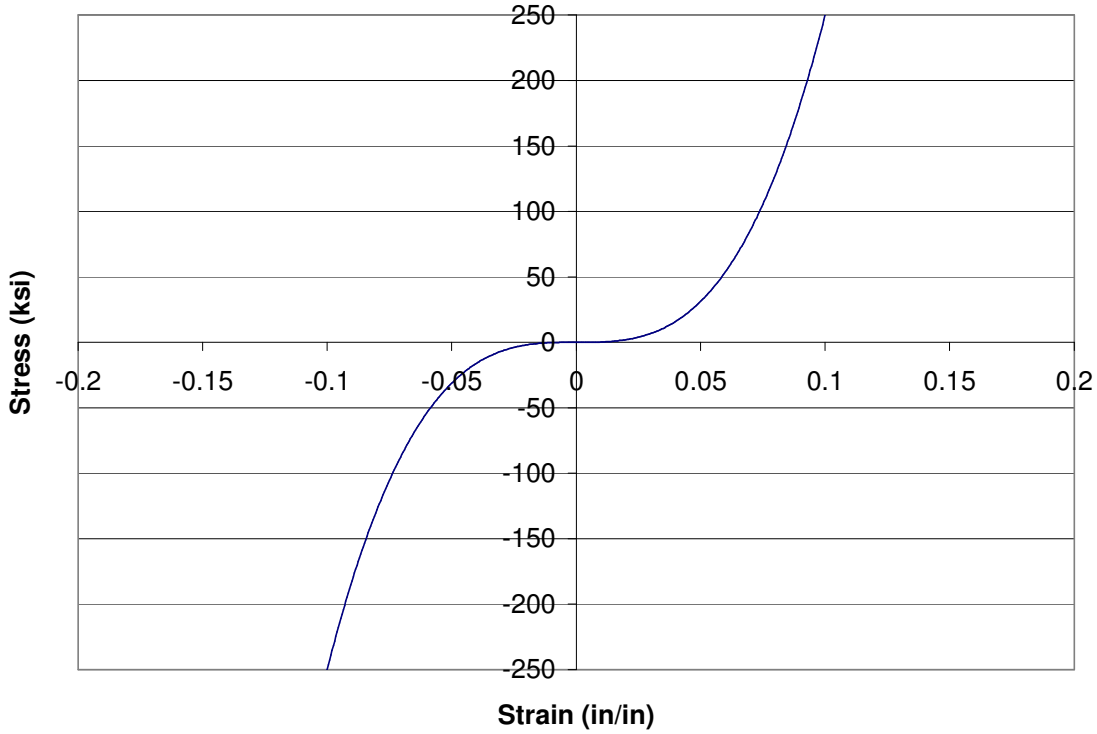

Figure 2.1 - Theoretical Hyperelastic Material Stress-Strain Behavior

From the initial report on hyperelastic element behavior (Jin, 2003), the results of single degree of freedom model were given for a wide range of hyperelastic behavior. The goals of the study were to examine the effects that the hyperelastic elements have on structural behavior in terms of maximum displacement, residual displacement, and maximum base shear. This study was completed using a combination of analysis routines in Matlab. Since no model correlation was performed in the initial report, the models were verified versus comparable Nonlin models before the hyperelastic elements were added. OpenSees has been used to reproduce these analyses and results such that the findings can be verified for the behavior of hyperelastic elements.

A range of 5 different sets of hyperelastic relationships were studied in an SDF model monitoring their effect on maximum displacement and base shear. Each of the 5 sets of equations represents a different ductility demand of the system, ranging from 2.5 to 7.5. Ductility demand is defined for a system as the ratio of the ultimate displacement where collapse occurs to the displacement at which first yielding occurs to. Higher ductility demands entail more inelastic behavior, while lesser demands describe a system that deforms less before ultimate failure.

The equations for each ductility demand were formed by fitting a cubic polynomial to a set of boundary conditions. The boundary conditions were established for the curves using yield strength, stiffness, and hardening ratio. Each hyperelastic material was installed into an SDOF frame in a bracing element and analyzed using incremental dynamic analysis. For each increment of ground motion used, the maximum displacement, residual displacement, and acceleration response history were recorded and used to produce the IDA curves for each model.

To fully evaluate the available range of behavior within each of the five ductility demands, a set of 8 equations were chosen in the initial hyperelastic study (Jin, 2003). A total of 40 model sets were analyzed using incremental dynamic analysis for the effect of hyperelastic elements on the system responses. Each equation represents a different type of hyperelastic stress-strain behavior, formed by fitting a curve to a set of constant boundary conditions. These equations are labeled F1 through F8, with F1 representing the linear behavior for the ductility demand, and F8 representing the relationship with the most curvature. The equations for a ductility demand of 2.5 are listed in Table 2.1.

Table 2.1 – Hyperelastic Functions for Ductility Demand of 2.5

	Hyperelastic Functions
F1	$988.27\ \delta$
F2	$8.25\ \delta^3 + 60.57\ \delta^2 + 790.62\ \delta$
F3	$19.80\ \delta^3 + 72.68\ \delta^2 + 691.79\ \delta$
F4	$44.54\ \delta^3 + 52.49\ \delta^2 + 592.96\ \delta$
F5	$82.49\ \delta^3 + 494.14\ \delta$
F6	$148.48\ \delta^3 - 121.14\ \delta^2 + 395.31\ \delta$
F7	$214.47\ \delta^3 - 242.27\ \delta^2 + 296.48\ \delta$
F8	$371.21\ \delta^3 - 605.68\ \delta^2 + 247.07\ \delta$

The structure used in Jin's study is an SDF representation of a 10 story, 3 bay system. The lateral stiffness and period of vibration for the SDF model match the values for the 10-story structure. For comparison of results, IDA curves were formed for each hyperelastic relationship and compared versus other relationships in the same ductility demand. The IDA curves show the progression of each response measure for the system

as it is subjected to increasingly intense ground motions. One ground motion was chosen, and scaled over the range of behavior from zero to three times the actual ground acceleration. This range ensures that inelastic behavior is achieved in the structure, giving a valid set of results for comparison of behavioral results between elements.

The results of the hyperelastic study by Jin show a range of structural behavior influenced by the inclusion of the hyperelastic devices. The results for both maximum displacements and the base shear were combined to determine which hyperelastic relationships result in the optimum behavioral benefit for the system. From these results, the most desired behavior was achieved using the F6 and F7 relationships from the ductility demands of 5 and 6. The overall behavior of the structure with hyperelastic elements indicated that the likelihood of structural collapse would be minimized while avoiding significant increases base shear. These results were shown to work best for this particular structure, and new relationships would clearly need to be evaluated for their effectiveness in different structural systems.

2.9 Other Types of Structural Devices

Several types of seismic protection devices have been studied for their effects on structures under dynamic loadings. The three principal types include seismic isolation devices, velocity dependent devices (dampers), and displacement dependent devices (braces). The overall goal of these devices in structural systems is to mitigate damage and reduce instability that can be caused by the inelastic deformations of a system subjected to strong earthquake ground motions. While structures are designed to perform inelastically under strong loadings, these devices account for extra life-safety and stability criteria such as improved energy dissipation and improved stability.

Energy dissipation devices are desirable because designing structures to behave elastically under all possible loading scenarios is economically infeasible. The structure would need to be several times stronger than standard design normally accounts for. The inclusion of seismic protection devices is often an economically viable solution that can provide a variety of significant influences on system behavior.

The effectiveness of structural devices comes from the reduction of the demand on a structural system to dissipate energy through repetitive inelastic deformations. This

reduction in system demand, however, may be accompanied by an increase in system forces. While a hyperelastic element would not be installed for the purposes of energy dissipation, it may reduce the likelihood of collapse under high P-Delta effects while contributing only a minimal increase in system forces while displacements are small. Therefore, the overall life safety and stability criteria are met using a device more sensitive to system forces at service level loads.

Of particular interest to the proposed research on hyperelastic devices is the research performed on nonlinear fluid viscous dampers in nonlinear dynamic analysis (Oesterle, 2002). This study shows that a nonlinear response of seismic protection devices is most efficient to dynamic structural response. Like hyperelastic devices, the increased effectiveness of the device as structural response increases shows improved efficiency for systemic influence. The stiffening dampers decrease residual displacement, as well as the amount of dispersion present in the IDA results. The modeling of hyperelastic devices involves the use of a similar type of increasing response in the hyperelastic material behaviors.

2.10 Scaling of Earthquake Records

Different means of applying intensity measures and of scaling seismic records will influence the structure's behavior and thus the effect of any devices being studied for influence on structural behavior. When already considering the natural randomness of seismic loading on structures, adding another possible source of error through uncertain scaling practices will compound the amount of variability (dispersion) in the final results of IDA analysis. By reducing the variability in the IDA curves, fewer records are required to achieve a given level of confidence in estimating the fractiles damage-values of limit-state capacities (Vamvatsikos and Cornell, 2002).

Nonlinear response is generally shown to give an unbiased response median when using scaling methods. Different ground motions are made to represent the same event through scaling in relation to their given magnitude (M) and distance (R). Normalized hysteretic energy (NHE) response is the only nonlinear response factor which is dependent on M and R (magnitude and distance), meaning that record scaling is not

without some errors (Shome, et al., 1998). Further investigation is warranted into the causes and influences of the hysteretic energy variability.

The use of a single spectral acceleration value may be appropriate for the first mode response of a structure, while higher modes may require two or three. As a structure becomes more damaged and moves into the nonlinear behavior region, period lengthening will cause the structure to be more influenced by its higher mode frequencies. A single spectral acceleration value which will keep dispersion at a minimum for a higher-mode structure occurs only within a very narrow range and is difficult to find as damage increases (Vamvatsikos and Cornell, 2002). Using a vector of intensity values is proposed as the solution to including multiple spectral values into an IDA procedure. A vector of two intensity values may be used, or a power-law combination of three values may be necessary for higher mode influenced structures. The use of three spectral accelerations increases accuracy even further. The dispersion between IDA records may be reduced by up to 50% by taking the elastic spectral information into account in the scaling methods used for the applied ground motion records.

By selecting an appropriate IM value on the basis of spectral shape for a given record, dispersion may be reduced and bring more accuracy/confidence in the use of IDA. The latest and most admissible methods of record scaling should be used to account for variability issues and to ensure the validity of the analysis results, as found in Shome and Cornell (1998) and Chapter 6 of (2002).

A study has been conducted considering the scaling of records, sensitivity of results to distance (R) and magnitude (M), accuracy of results given a limited number of records, and the amount of scatter in results (Shome, et al., 1998). The study considers multiple damage measures as representative of modern building demands (ductility, normalized hysteretic energy (NHE), damage indices, and global factors). The median values attained using the four bins of ground motions are compared to find the behavioral correlations. The scaling is achieved using a representative ground motion attenuation law.

Based on the normalized nonlinear results of a single MDOF structure without high mode effects, the conclusion is reached that the scaling of records to match the bin median spectral acceleration results in unbiased estimates of the response medians and

reduced variability. Based on constant spectral acceleration (S_a) values, the conclusion is reached that there is no dependence on M or R for the median nonlinear response values, with the exception of NHE. (Shome, et al., 1998)

2.11 Dynamic Behavioral Uncertainty

Due to discrepancies between modeled systems and real structures as they exist, analytical scenarios exist which include uncertainty in the final results as they pertain to actual building behavior. This concept is the basis for use of probabilistic applications to dynamic structural analysis. While IDA is a powerful and informative analysis type for seismic analysis, it cannot accurately portray exact building behavior due to the randomness contained within the analysis parameters. Actual soil and ground motion characteristics can lead to behavioral uncertainty which may not be correctly accounted for within a specific analysis. Behavioral uncertainty can not be measured through analytical uncertainty like IDA curve dispersion; however, it can still influence the correlation between analytical results and the actual dynamic response of a structure.

Soil characteristics are influential in how a seismic ground motion is transferred as lateral forces into a structure. Variable soil properties will influence the magnitude and characteristics of any seismic ground motion because the soil is the medium through which earthquake loadings are transferred into a structure. This concept is not to be confused with soil-structure interaction, which describes the dynamic behavior of soils and structures as a combined system. Soil properties are known to greatly influence how the ground acceleration is propagated to a structure. Sites with loose soil may experience great magnification, while sites with more fractured rock characteristics may inhibit wave propagation. Thus, a large amount of variability exists regarding the actual ground acceleration a structure will experience. This is the basis for the formation of the seismic design spectra implemented by NEHRP (FEMA 2000) and ASCE7 (ASCE 2002). Further research in this topic of variability may increase the understanding of how geotechnical factors influence the behavior of structures and certainty of dynamic structural response.

Motion characteristics are also influential on the effect of a seismic event on a structure. While a new earthquake may have similarities with other earthquakes, no two

records contain the same combination of intensity, duration, frequency content, and direction. This type of variability may not be accounted for through standard scaling and deterministic analytical procedures. Investigation of these uncertainty aspects of dynamic analysis requires the use of high levels of computing power to increase the accuracy of results, as well as probabilistic measures to account for uncertainty and unpredictability. Probabilistic measures are present in the creation of the design spectra used in the current building provisions given by NEHRP (FEMA, 2000).

Chapter 3 - Hyperelastic Behavior

3.1 Introduction to Hyperelastic Behavior

While many different types of structural devices have been studied for their effects on the dynamic behavior of structures, there are still numerous disadvantages associated with some of the device properties. Rigid bracing results in a detrimental amount of system forces at service loads, and dampers are ineffective at stabilization for high levels of displacement. New device characteristics are under investigation for optimizing structural efficiency by controlling dynamic behavior while minimizing behavioral disadvantages. Devices exhibiting hyperelastic behavior were chosen for this investigation due to their theoretical contribution to structural behavior. The inclusion of hyperelastic behavior in a structural device introduces new benefits for the engineering of structures under dynamic loadings.

3.2 Constitutive Properties of Hyperelastic Materials

Hyperelastic materials behave elastically along a nonlinear stress-strain curve and are defined for the purposes of this research by a cubic polynomial relationship for the force and deformation of the related element. A desired force-deformation relationship may be formed for a hyperelastic element based on the parameters of a structural system and converted to the associated hyperelastic material behavior. The material is designed to gain stiffness as the deformation increases on the device.

The theoretical function of braces with hyperelastic material properties is to add increasing stiffness to a structure as deformation increases. Hyperelastic behavior may prevent instability and increase structural predictability at high levels of acquired displacement in a structure. Similar studies have been performed on other nonlinear seismic devices such as dampers; however, a purely elastic nonlinear response has not been evaluated for the influence on structural behavior.

3.3 Benefits of Hyperelastic Devices

Hyperelasticity is useful in increasing structural stability while avoiding increased base shear that often occurs with linear stiffening devices at lower ranges of deformation. Under a given ground motion, devices that add stiffness will induce stronger vibrations and increase the base shear demand by reducing the period of vibration. If stronger vibrations are instilled into a structure, then the structural strength must be increased. Increased strength requirements result in an unacceptable performance where the braces are designed to be beneficial.

However, the material behavior of hyperelastic braces makes it possible to provide varying amounts of stiffness to a structural system based on system demand. A hyperelastic brace is designed to minimize the increase of base shear demand when the structural displacements are small through the low initial stiffness prescribed by the cubic polynomial. At higher levels of deformation, the stiffness of the brace increases and adds stabilizing forces to the system.

Stability is the main concern in a structure where high levels of displacement occur under a ground motion. Also, lengthening of structural period of vibration occurs as yielding takes place in a structure and the elements lose stiffness. This behavior is visible in a static pushover curve when it starts to bend over after yielding occurs. The bend in the static pushover curve indicates that the structural stiffness is decreasing as structural members become less effective at resisting the system loads. A hyperelastic device can be prescribed by a specific polynomial behavior that would be most influential on a system during the loss of strength well beyond yielding. Essentially, a hyperelastic brace will replace the stiffness response of the yielded members. This type of structural device, like the nonlinear hardening dampers (Oesterle, 2002), may be expected to increase structural stability by controlling the yielding response of a structural system.

A hyperelastic structural device may also be expected to reduce the amount of dispersion present in the results of a structural analysis found using incremental dynamic analysis. This is because as the yielding response of a structural system becomes more controlled, the behavior becomes more predictable. Incremental dynamic analysis will give a range of insight into the behavior of structures with yielding behavior. Systemic factors such as yield sequence and lengthening of structural period of vibration will be

directly influenced by the properties of the brace due to the specific design for influence on the yielding response of the structure. The braces are designed to increase the structural predictability as yielding occurs and therefore reduce the behavioral variances associated with yielding.

3.4 Formation of Hyperelastic Equations

The polynomial force-deformation equations are formed by fitting a cubic polynomial to a set of boundary conditions based on system parameters. The boundary conditions are established for the curves based on ductility demand, yield strength, stiffness, hardening ratio, and curvature. These parameters form the basis for the behavioral characteristics of a hyperelastic material curve. The ductility demand is perhaps the most influential on hyperelastic behavior modeled by a cubic polynomial, and it is defined as the ratio of the maximum expected inelastic displacement versus the initial yield displacement. System parameters may be mixed with the desired curvature coefficients to form specific curvature relationships for hyperelastic behavior. A general form of a hyperelastic polynomial is given as follows:

$$F(x) = ax^3 + bx^2 + cx + d \qquad \text{(Equation. 3.1)}$$

where F is the material force, x is the displacement of the material, and the coefficients a, b, c, and d are the coefficients formed by the equation fitting process.

Varying ranges of curvature in the hyperelastic polynomials will affect how influential a hyperelastic material is at specific ranges of displacement. Low amounts of curvature result in a more linear-elastic type of behavior that is more influential at lower ranges of displacement. Higher amounts of curvature are more effective as displacements become closer to the yield point, and thus are most effective in systems where the behavior is expected to go beyond the yield strength.

Hyperelastic behavior entails specific relationships for material behavior that are reflected by the boundary conditions for the material properties. Once the stiffness, ductility, hardening ratio, and yield strength are established for a system, the boundary conditions can be found to manipulate these properties into the polynomial equations.

The boundary conditions are formed based on maximum system force, maximum displacement, and the slope at specific points of the curve. The boundary conditions for fitting a hyperelastic polynomial are shown in Figure 3.1, and the arrow indicates the shape of the hyperelastic equations as the curvature is increased.

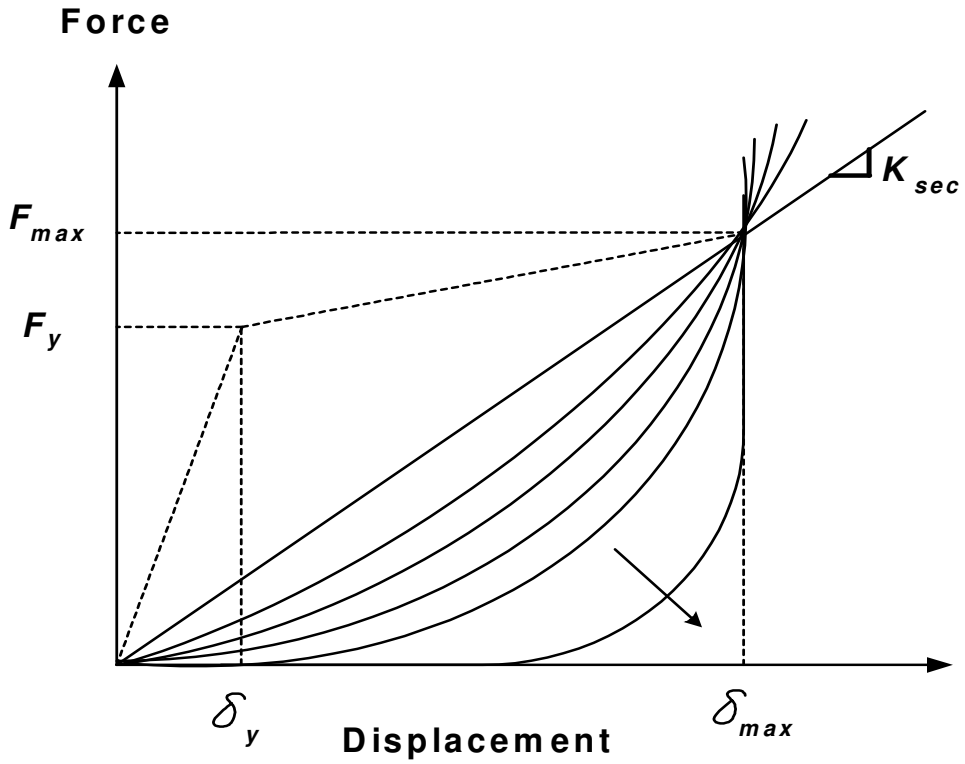

Figure 3.1 – Boundary Conditions for Various Types of Hyperelastic Polynomial Relationships

The curvature of the hyperelastic curve at any given point is based on the secant stiffness and slope coefficient for the particular curve. Varying the slope coefficients will instill a range of curvature relationships between the boundary conditions. Using this idea, ranges of hyperelastic equations may be formed for the same ductility value and set of structural parameters. Varying sets of hyperelastic equations are beneficial for determining the specific curvature relationships that are most beneficial for a specific structural system.

3.5 Programming Hyperelastic Behavior into OpenSees

In creating the new program files for the hyperelastic material as a uniaxial material in OpenSees, specific constitutive properties must be accounted for in the programmed files to get the correct material behavior. OpenSees reports stress and strain per time step of analysis for a uniaxial material. However, the hyperelastic behavior is defined in terms of a cubic equation for force and deformation for an element. Therefore, the known force-deformation relationships for a hyperelastic element must be converted to a stress-strain relationship to get hyperelastic material behavior. The polynomial relationship is defined for the uniaxial material in OpenSees the same as shown for the general hyperelastic polynomial relationship (Equation 3.1).

Relating material behavior to element behavior is crucial to establish the correct hyperelastic behavior. Setting the element area of a hyperelastic element equal to 1.0 accounts for the conversion of force to stress. This must be done by the user in OpenSees when the hyperelastic element is formed. Length has been included in the command for the material, and it is multiplied into the behavioral definitions of the hyperelastic material in the programmed files to account for the conversion of displacement to strain. The command line for the programmed material in OpenSees is as follows:

```
uniaxialMaterial Hyperelastic $Mattag  $A  $B  $C  $D  $L
```

where $Mattag is the material tag number, $A, $B, $C, and $D are the polynomial coefficients from the fitting process, and $L is the length of the element to which the hyperelastic material will be assigned. The C++ code files for the formation of the hyperelastic material in OpenSees may be found in Appendix C.

This material behavior is validated by subjecting an element with an assigned hyperelastic material to a ground motion in OpenSees and graphing the observed force-deformation behavior. The length of the element must be input when the hyperelastic material is defined, and the area of the element is set to 1.0. The observed force-deformation behavior of the hyperelastic element under the El Centro ground motion exactly matches the cubic polynomial equation, as can be seen in Figure 3.2. Correlation

between the material behavior and the material equation will not occur if the force-deformation behavior for the element is not properly converted to the stress-strain behavior for the material.

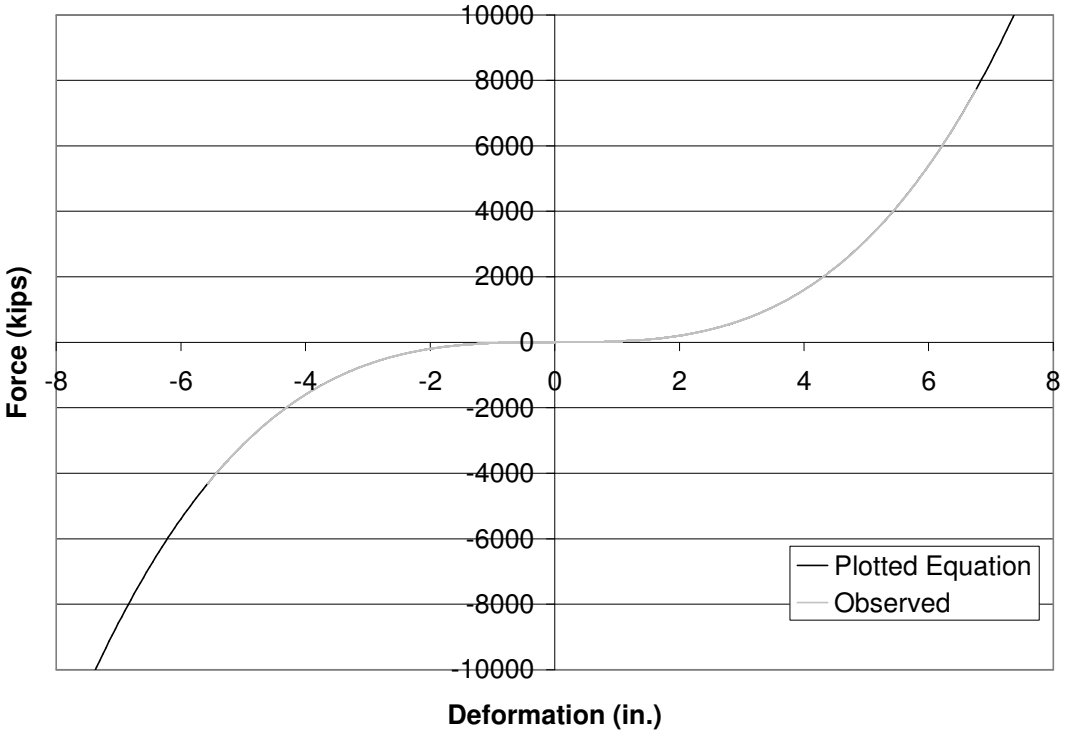

Figure 3.2 – Observed Hyperelastic Element Response versus the Polynomial Expression

3.6 Verification of Hyperelastic Programming

After the hyperelastic material has been successfully programmed into Opensees, verification must be performed on the material to ensure that it gives the desired behavior. Verification of the hyperelastic material properties is crucial before the material can be used to study the effects of hyperelastic braces on structures. Since the new material added to OpenSees has not been verified prior to the research, models need to be analyzed to establish information that correlates the accuracy of the programming before more complex analyses are pursued.

To perform the verification of this new material, a complete set of models was established using a range of hyperelastic polynomials, and the results are compared to the expected behavior. The expected behavior was established from a hand made Newmark

analysis routine in MathCad (2001) that accounts for nonlinear material behaviors such as hyperelasticity in elements. Most analysis software packages are not capable of analyzing such a specific type of nonlinear material; however, since this Newmark package is hand made, it can account for any type of nonlinearity the user desires.

The models were all SDOF models with constant stiffness, mass, and yield strength such that the hyperelastic material behavior is isolated between the models. Matching results for the behavior of a hyperelastic material are found between OpenSees and the Newmark routine, and thus verify that the hyperelastic material is accurately given by the OpenSees model. Also, equilibrium is satisfied by both solutions for the hyperelastic element, and since there is a unique equilibrium response for any structural system under the same loading, then the hyperelastic material behavior must be correct.

Once the material behavior is verified versus the Newmark routine, more hyperelastic models are analyzed and compared to results from a previous report on hyperelastic devices. More complete details regarding the models and the verification of the hyperelastic material, including the Newmark routine created in MathCad, may be found in Section 3.1 of Appendix B.

3.7 Hyperelastic Relations used for Research

The hyperelastic equations used for the analysis of the MDOF structure described in detail in Chapter 4 are formed using the system parameters of the structure to which they will be applied. One brace will be installed per level of the structure, and the equations will be formed based on the secant stiffness, yield force, ductility, and hardening ratio from the structure. These parameters form the boundary conditions to which the hyperelastic polynomials can be fit according to the prescribed ductility. The displacement-based parameters will be considered on a per-story basis rather than for the entire system since the elements will be installed per level of the structure.

Based on the recommendations from the previous research performed by Jin, curvatures of 0.3 were used in fitting the hyperelastic equations to the boundary conditions. Two sets of equations were formed for analysis in the MDOF model based on two different ductility ranges. This is necessary to evaluate the effectiveness of a range of hyperelastic elements under a range of performance criteria. Further explanation

of the system parameters used for the hyperelastic equation fitting, as well as the modeling process used for the hyperelastic elements, may be found in Section 6 of Chapter 4.

Chapter 4 - 6-Story Analytical Model

4.1 – Introduction to the Modeling

To fully assess the performance of hyperelastic braces for their stabilizing potential, a model of a 6-story structural steel moment resisting frame with braces installed is created using OpenSees. The properties of the model are modified such that P-Delta effects create a more drastic reduction in secondary stiffness. Due to these modifications, the structure will fall short of several performance expectations. Two sets of hyperelastic braces are installed to analyze the responses with varying brace characteristics and to improve the life-safety performance criteria of the structure. The structure created for the analyses is created as a duplication of the model described in Chapter 3 of *BSSC Guide to Application of the 2000 NEHRP Recommended Provisions* (Charney, 2003).

Several types of analytical techniques were employed in the course of analyzing the performance of this structure. To assess the initial strength and stability of the structure, nonlinear static pushover analysis of the structure was performed. Nonlinear dynamic analysis was performed using two different ground motions to analyze the dynamic behavior of the frame. Finally, to compare the performance of the structure under increasing ground motion intensity, incremental dynamic analysis was performed on the structure for the two ground motions.

The objectives of the analyses are to investigate the effectiveness of the hyperelastic braces at enhancing the stability of the structure and the corresponding effects the braces have on system forces. The stabilization of the structure will be judged based on the amount of interstory drift acquired with and without hyperelastic bracing during specific ground motions that incite an unstable response from the structures. The effectiveness of the stabilization will be based on a comparison of the drift behavior versus the related increase in base shear.

4.2 – Description of the Structure

The structure chosen for the advanced analyses of hyperelastic braces is an MDOF 6-story office building located in Seattle, Washington. According to the seismic provisions under which the structure was designed, the building is assigned to Seismic Use Group 1 with an Importance Factor of 1.0. The lateral load resisting system consists of steel moment frames around the perimeter of the building. In the N-S direction there are five bays at 28 ft on center, and the frames in the EW direction consist of six bays at 30 ft on center. The story heights are 12 ft-6 in, with the exception of the first floor which has a height of 15 ft. There is a parapet at the roof level that extends 5 ft above the roof level, and there is one basement level that extends 15 ft below grade. The analysis of the structure assumes a fixed base condition resulting from the columns of the moment frames being embedded into pilasters formed into the basement walls. Figures 4.1 and 4.2 show the plan and profile views for the N-S moment resisting frame.

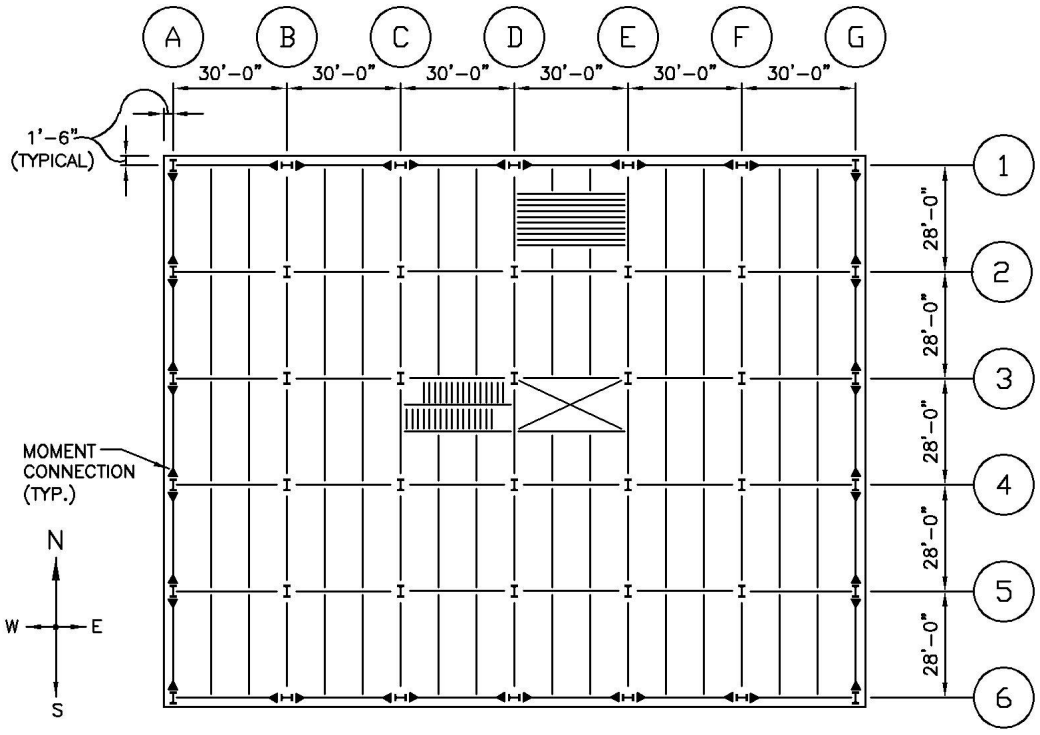

Figure 4.1 – Plan View of Structural System

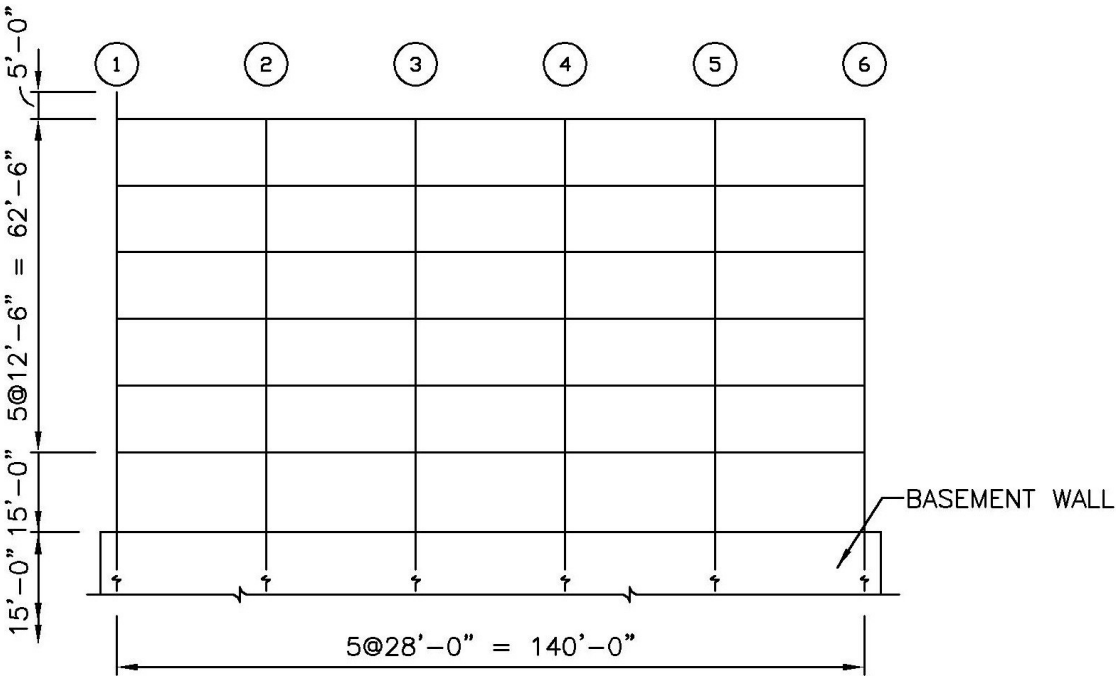

Figure 4.2 – Elevation View of Structural System

The model created for analysis in OpenSees consists of the moment resisting frame of this structure in the N-S direction. For this frame, all of the columns bend about their strong axes, and the girders are connected with fully welded moment connections. The design of these connections is assumed to be constructed according to post-Northridge protocol. All of the analyses considered for this structure will be for the lateral loads acting on the N-S moment frame. Analysis for the E-W frame direction would be performed in a similar manner.

All of the interior columns are designed as gravity columns and are not intended to resist any of the lateral loads. However, some of these columns may be engaged by the hyperelastic braces that will be added to the frame. These columns are assumed to be part of an interior corridor that would be designed to remain elastic due to the local forces introduced by the braces.

The design of the frame in the NS direction was performed in accordance with the *Seismic Provisions for Structural Steel Buildings* published by the American Institute of Steel Construction (AISC, 2002). All members and connections are designed using steel

with a nominal yield stress of 50 ksi. All of the selected members meet the width-to-thickness requirements for special moment resisting frames. Also, the size of the columns relative to the girders ensures that plastic hinges will form in the girders before forming in the columns. Table 4.1 summarizes the members selected for the N-S moment resisting frame.

Table 4.1 – Selection of Members for the N-S Moment Frame

Member Supporting Level	Column	Girder	Doubler Plate Thickness (in)
Roof	W21x122	W24x84	1
6	W21x122	W24x84	1
5	W21x147	W24x84	1
4	W21x147	W24x84	1
3	W21x201	W27x94	0.875
2	W21x201	W27x94	0.875

Doubler plates are used at each of the interior beam-column joints to provide adequate strength through this region. Plates with a thickness of 0.875 in. are used at levels 2 and 3, and plates with a thickness of 1.00 in. are used at levels 4, 5, 6 and R. The doubler plates are only installed on the interior joints, and no doubler plates are used in the exterior beam-column joints.

4.3 Modeling of the Structure

Several techniques are employed in the creation of this model to accurately represent the nonlinear behavior. The techniques used to model the beams and the beam-column joint regions are created to explicitly replicate the expected yielding behavior of those elements. The use of elastic and inelastic elements is combined with zero-length rotational elements to create assemblies that replicate the desired strength behavior of the components of the moment frame.

As mentioned previously, the model is replicated from a model created by Charney (2003) for analysis of the 2000 NEHRP provisions. Models were originally

created and analyzed using the Drain-2DX analysis package in that reference. These models were obtained and used for comparison in creating the new model in OpenSees to ensure that the structure is recreated accurately.

Nonlinear analysis of a complex structure is an incremental process that requires attention to many details. To replicate a nonlinear model between two separate programs, linear analysis should be performed first to compare the basic information for the expected behavior. Once agreement is reached on the linear analysis, the nonlinearities should be introduced incrementally to ensure that each source is accurately included into the model. This approach is used in the creation of the OpenSees model from the Drain-2DX model.

In the modeling of the structure, no shear deformations are included in the behavior of the elements. The yielding of the structure is concentrated in the girders and the panel zone regions of the structure. Centerline dimensions are used for the alignment of the elements, and no rigid end zones are installed. Composite action between the beams and the floor slabs is ignored. P-Delta effects and damping are included in the model through the use of a separate ghost frame. Later, the ghost frame will also be used to include the hyperelastic braces into the system.

Zero-length spring elements and compound nodes are employed in the modeling of this moment resisting frame to represent yielding locations within the frame. The yielding occurs at designated plastic hinge locations in the girders, and in the panel zone regions for beam-column connections.

A compound node consists of a pair of single nodes that share the same spatial coordinates. The X and Y degrees of freedom of the first node are constrained to the X and Y degrees of freedom of the second node, creating a slave and master node hierarchy. The compound node has a total of four degrees of freedom: an X displacement, a Y displacement, and two independent rotations. To create the yielding behavior using a compound node, one or more rotational springs can be installed between the two nodes using a zero-length element. The spring provides moment resistance in proportion to the moment created by the relative rotation between the two nodes. Without a spring, the node acts as a moment-free hinge. Bilinear material behavior is assigned to all of the spring materials in the model for yielding. A typical compound node with a rotational spring is shown in Figure 4.3.

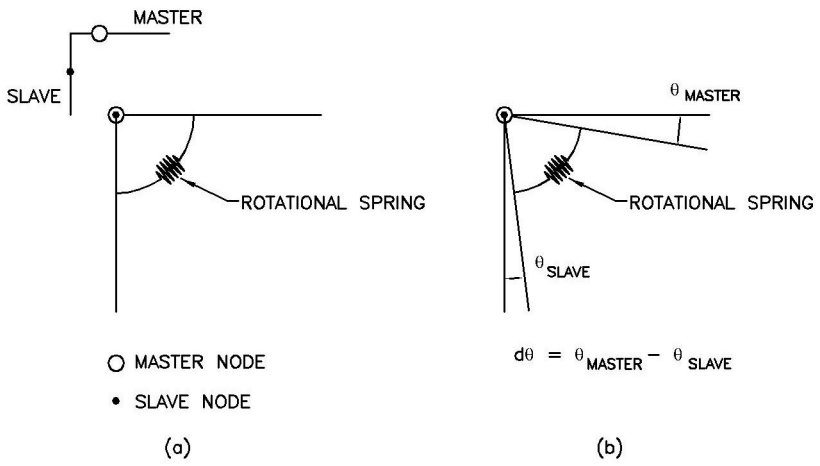

Figure 4.3: Typical Compound Node (a) Undeformed and (b) Deformed

Using an assembly of compound nodes, the nonlinear behavior of the panel zones and the girders of the structure can be modeled. A typical panel zone assembly consists of 4 compound nodes and two rotational springs per panel zone, with eight rigid links between the nodes. A typical girder consists of one compound node at each end of the girder to represent plastic hinges. A detail of a girder and the connection to two interior columns is shown in Figure 4.4.

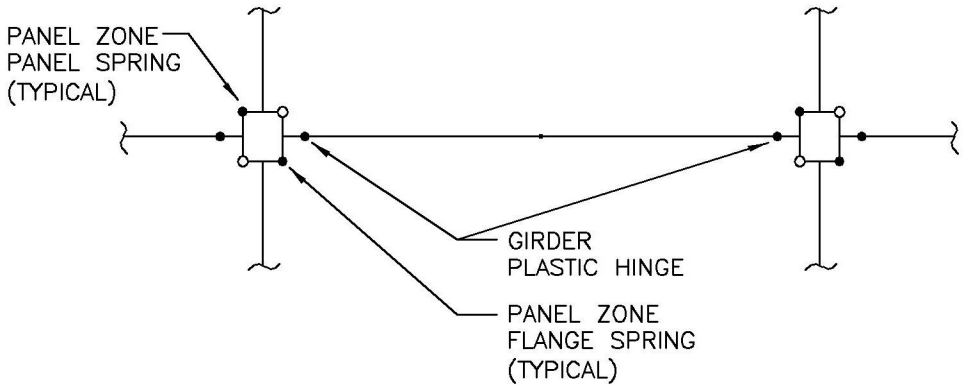

Figure 4.4: Typical Girder and Column Assembly

The total amount of story drift for a moment resisting frame under dynamic loading may be significantly influenced by the deformations that occur in the panel zone region of the beam-column joint. For this model, the panel zones are constructed using the compound nodes previously described with rotational springs to implement an approach developed by Krawinkler (Downs, 2002), (Krawinkler 1978). While the model

is conceptually simple, the disadvantage occurs in the number of degrees of freedom required.

The Krawinkler model assumes that the panel zone area has two mechanisms that act in parallel and contribute lateral resistance. The shear resistance of the web constitutes one mechanism, and it is modeled by the properties given to one of the rotational springs in the panel zone model. The flexural resistance of the flanges is the second mechanism, and it is modeled by the second rotational spring in the panel zone. The derivation of the spring values is contingent on the element properties framing into the panel zone. Therefore, different spring values occur as the beams and columns change within the frame, and different values occur between interior and exterior panel zone connections.

The girders are modeled in a similar way to the panel zones to include plastic hinge regions for yielding. This frame is designed according to the strong-column/weak-beam principle, so the girders are expected to yield in flexure before any column yielding occurs. The portion of the girder between the panel zones is modeled as a total of four segments. There are two compound nodes near the ends of each girder, and a simple node at midspan to enhance the deflected shape of the structure. Typically, a plastic hinge will grow in length as yielding progresses in a girder. Modeling of this behavior, however, is outside of the capabilities of this analysis. The spring properties are assigned for each girder type based on the moment-curvature analysis of the particular cross section. Two springs are installed between each compound node in a girder to model the separate yielding properties that are present at each plastic hinge location.

The columns of the moment resisting frame are input as elastic elements in the OpenSees model pinned at the base of the structure. This is consistent with the strong-column/weak-beam design principle and simplifies the modeling process for the purposes of this project. Column yielding is shown to occur in the model analyzed by Charney (2003); however, the influence is not as significant as the panel zone and girder yielding. The main behavioral parameters of the frame can be analyzed under the hyperelastic braces just as effectively with elastic columns. The elements of the Drain-2DX model were changed to elastic elements for model verification. The columns were not modeled as yielding elements in either program due to modeling inconsistencies between the

software. Drain-2DX models column yielding through a biaxial interaction diagram; however, this option is not yet available in OpenSees.

The damping for the frame is included through the use of a ghost frame in the modeling setup. This is a fictitious frame connected to the side of the moment frame using rigid links. The ghost frame is fully hinged through the interior and pinned at the base, and only provides the properties of damping and P-Delta effects into the moment frame. Separate viscous dampers are installed in the ghost frame to represent the mass-proportional and stiffness-proportional components, respectively. These components are calculated based on the Rayleigh proportional factors taken from the Drain-2DX model of the frame, and represent a total of 3% of critical damping. Figure 4.5 shows the moment resisting frame displayed with the ghost frame.

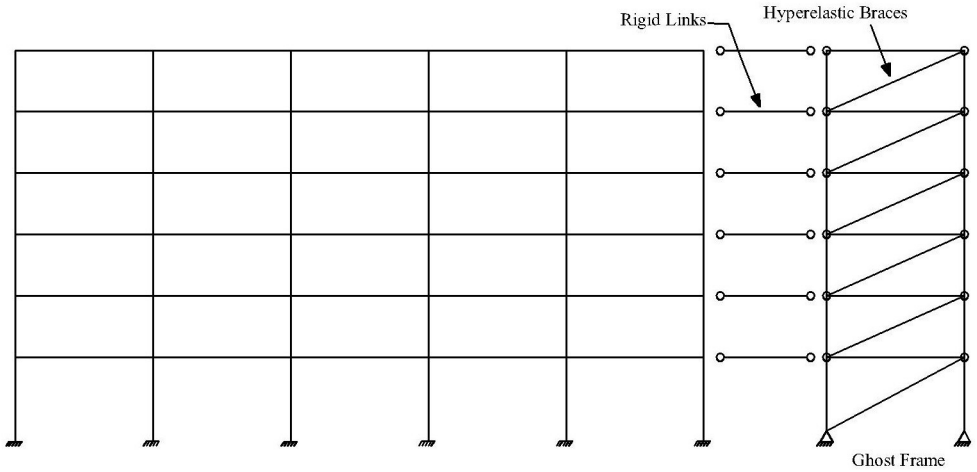

Figure 4.5 – Moment Resisting Frame with Ghost Frame

P-Delta effects are included in the analysis of the moment frame, and are a key property used to attain dynamic instability. The negative stiffness effects provided by these second-order effects are input on the ghost column as additional vertical loads. These vertical loads are influential on any amount of lateral deformation in the structure, and increase the amount of drift based on the magnitude of the vertical loading. High levels of P-Delta effects are added into the structure to create two separate post-yield strength scenarios for analysis of the hyperelastic braces.

4.4 Model Verification

To verify that the newly created model in OpenSees behaves the same as the model created by Charney, a modal analysis was performed on the two structures. For all of the analyses performed, all element loads were removed to avoid any inconsistencies that may occur in load application between the two programs. OpenSees and Drain-2DX do not model element forces using the same methods, so these loads were removed for the sake of simplicity and to avoid another round of model verification.

Using the modal analysis functions of both programs, the models are found to correlate for the first 5 modal periods of vibration. Any higher modes were deemed unnecessary. Table 4.2 lists the resulting periods of vibration from the two programs for the moment resisting frame models.

Table 4.2 – Modal Periods of Vibration for the Moment Resisting Frame

Mode	Period of Vibration, OpenSees	Period of Vibration, Drain-2DX
1st	1.87194 sec	1.8720 sec
2nd	0.60204 sec	0.60206 sec
3rd	0.31270 sec	0.31271 sec
4th	0.19118 sec	0.19118 sec
5th	0.12793 sec	0.12793 sec

Further verification was performed by subjecting both models to the El Centro ground motion using the respective programs in which they were created. The displacement and acceleration response histories were verified as accurate within 1% at the peak values of the responses between the two programs. The displacement response histories for the two programs under the El Centro ground motion are given in Figure 4.6

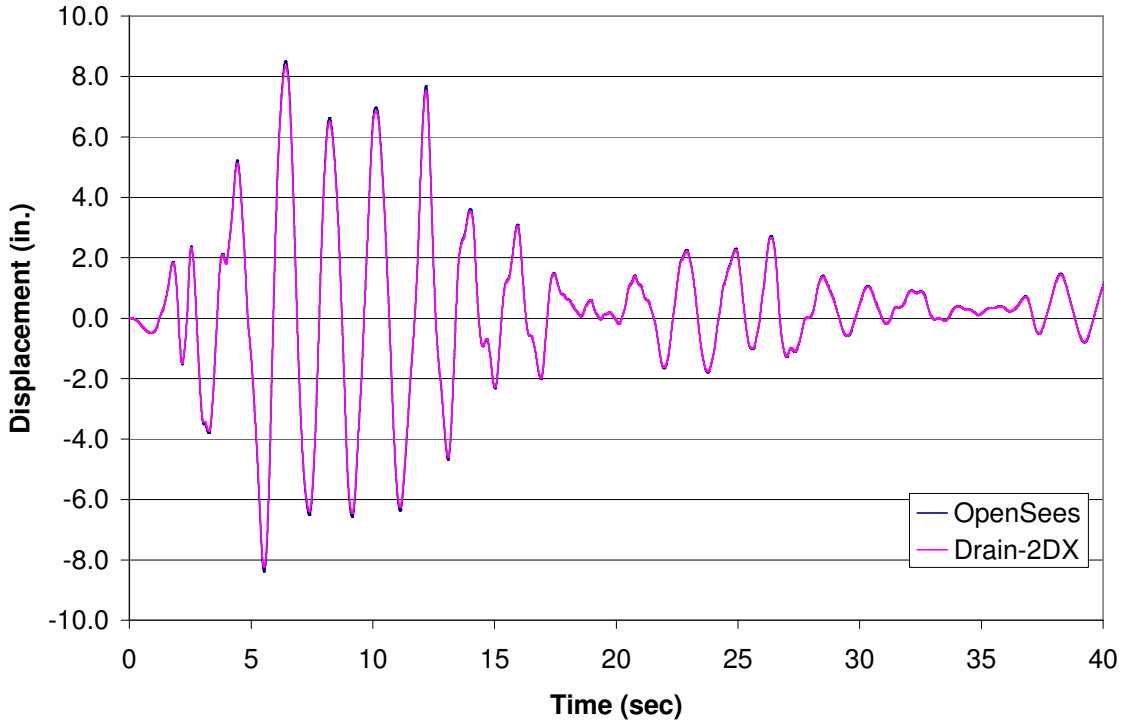

Figure 4.6 – Displacement Response History of Moment Frame under El Centro Ground Motion from Both Software Packages

4.5 Important Behavioral Parameters

Once the model was established as being accurate in OpenSees, the properties of the moment frame were analyzed using a static pushover analysis to determine the yielding sequence and post-yield strength properties of the frame. Two sets of increased P-Delta forces were added onto the ghost frame to create two post-yield strength scenarios that may induce dynamic instability into the structure. The pushover curves for the two P-Delta cases are shown in Figures 4.7 and 4.8. The P-Delta cases are created as multiples of the P-Delta loads created for the original structural analysis in Nonlin

The second P-Delta case is of particular concern due to the negative post-yield strength of the structure. This case would be most likely to generate poor dynamic performance after yielding occurs during a seismic event, and creates the best case scenario for determining the stabilizing effectiveness of the hyperelastic braces. Both P-Delta cases are used to evaluate the effectiveness and performance characteristics of the braces.

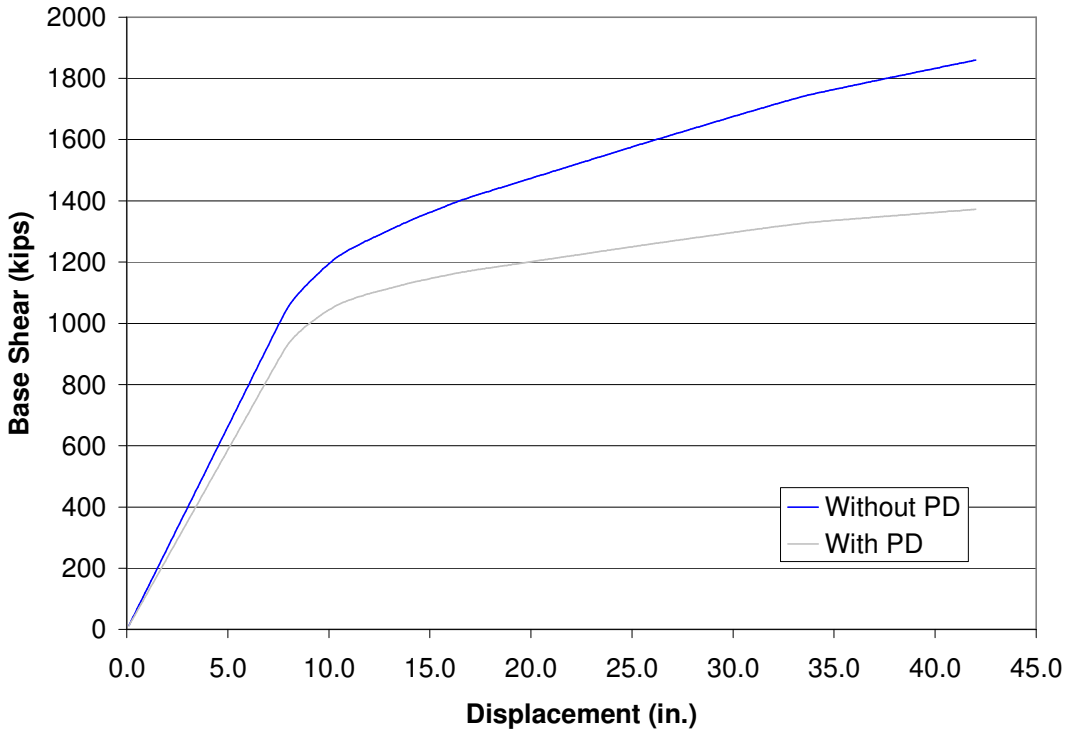

Figure 4.7 – Pushover Curve for First Case P-Delta Effects

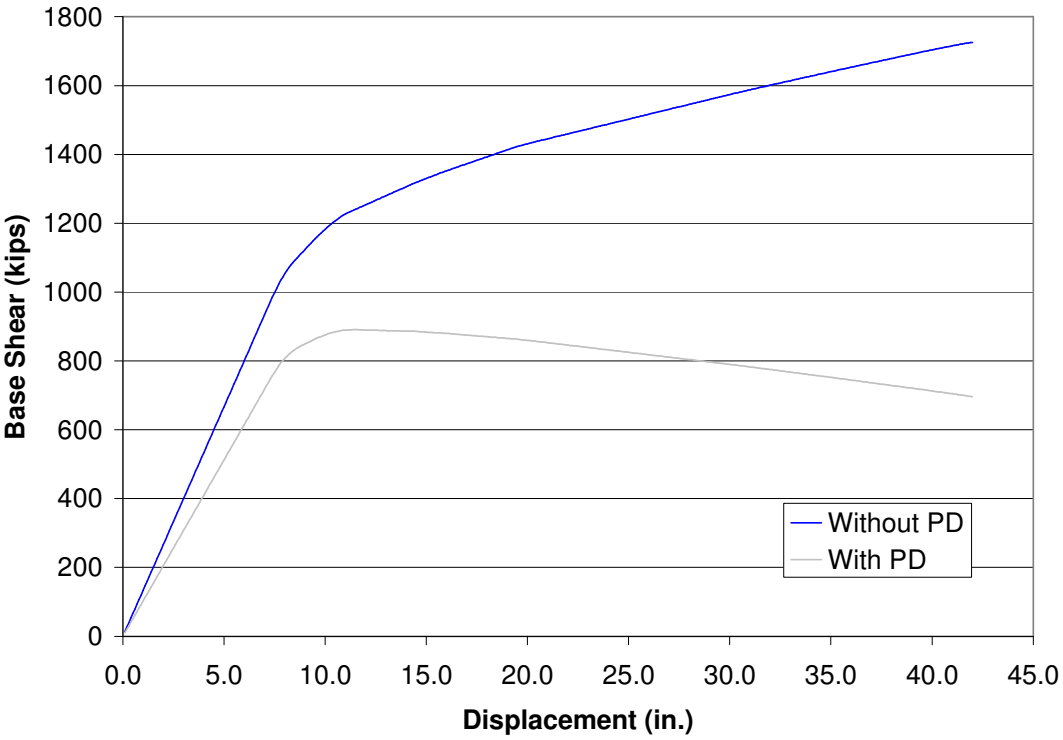

Figure 4.8 – Pushover Curve for Second Case P-Delta Effects

The two P-Delta cases result in dynamic behavior for the frame that is the idealized target for the application of hyperelastic braces. While the stability ratio produced by the vertical P-Delta loading may not represent a realistic loading case for a structure, the net effect of the geometric stiffness on the system creates a realistic problem that could exist in a structure. The stability ratio is calculated as shown in Equation 4.1, where θ is the stability ratio, P is the vertical load on the bottom level of the structure, H is the height of the bottom story, and K_E is the elastic stiffness of the system.

$$\Theta = \frac{P}{H} * \frac{1}{K_E} \qquad \text{(Equation 4.1)}$$

The relatively high period of vibration (more flexibility) of the frame makes it more sensitive to high ground motion intensities, and creates a structural scenario of real concern when coupled with the low post yield strength of the system. Structures with this amount of sensitivity and instability demonstrate a shortfall in life safety criteria due to the likelihood of collapse after yielding occurs.

4.6 Hyperelastic Braces

The hyperelastic relationships chosen for use in the moment resisting frame are based on the system parameters evident in the pushover curves. The hyperelastic curve equations are fitted to a list of boundary conditions including system yield strength, ductility, hardening ratio, and curvature. The secant stiffness is also used as one of the hyperelastic parameters, and it is based on the initial system stiffness and the maximum displacement expected for the system.

The equations are given in Tables 4.3 and 4.4 for both sets of braces used in the analyses. The equations are labeled F1 through F6 for the first through sixth floors, respectively. The equations are formed individually for each level based on the amount of interstory drift that the story is expected to experience. Therefore, each story has a specifically designed hyperelastic brace. The braces are installed in the ghost frame of the moment frame model to avoid any local effects the braces may introduce to the columns. This gives the same results as if the braces were to be applied to an interior

corridor of a structure that is designed to remain elastic over the range of local forces introduced by the braces.

Two different sets of hyperelastic relationships are developed for analysis in the moment resisting frame. The first set displays higher early stiffness, and may be theoretically effective in a system at lesser amounts of deflection. This set of braces is referred to in the analyses as Hyper 1. The second set of hyperelastic equations develops stiffness at a higher amount of acquired displacement and may be most applicable to systems that behave over a larger ductility range. The second set is referred to as Hyper 2 in the analyses.

The important behavior of both hyperelastic equation sets is based on the range of stiffening. This dictates at what point in the system's behavior the hyperelastic brace begins to add significant stiffness to the system. The net effect of the array of hyperelastic braces is to increase the system strength at the displacement range where P-Delta effects become detrimental. The effects of the hyperelastic braces on system stiffness can be seen in the pushover curves for both P-Delta cases in Figures 4.9 and 4.10. The new curves are plotted versus the old pushover curves to demonstrate how the hyperelastic braces overcome the negative geometric stiffness contributed by the P-Delta effects, and result in more system strength at high displacement levels. Also, any negative post-yield stiffness is avoided, resulting in increased stability.

Table 4.3: Hyper 1 Brace Equations

$F1 = 65.53\delta^3 - 187.2\delta^2 + 300.9\delta$
$F2 = 31.27\delta^3 - 114.4\delta^2 + 235.29\delta$
$F3 = 31.27\delta^3 - 114.4\delta^2 + 235.29\delta$
$F4 = 31.27\delta^3 - 114.4\delta^2 + 235.29\delta$
$F5 = 65.53\delta^3 - 187.2\delta^2 + 300.9\delta$
$F6 = 303.0\delta^3 - 519.5^2 + 500.91\delta$

Table 4.4: Hyper 2 Brace Equations

$F1 = 13.92\delta^3 - 39.77\delta^2 + 63.91\delta$
$F2 = 6.66\delta^3 - 24.37\delta^2 + 50.13\delta$
$F3 = 6.66\delta^3 - 24.37\delta^2 + 50.13\delta$
$F4 = 6.66\delta^3 - 24.37\delta^2 + 50.13\delta$
$F5 = 13.92\delta^3 - 39.77\delta^2 + 63.91\delta$
$F6 = 64.07\delta^3 - 109.83\delta^2 + 105.91\delta$

In the analytical process for the moment frame, the two sets of hyperelastic equations are applied to both P-Delta cases to establish a range of applied behavior for the devices. The first set of hyperelastic equations represents relationships for a more realistic amount of deflection in a system and therefore may be more applicable to actual building scenarios. However, the second set of hyperelastic equations may also be

applicable to certain dynamic cases. The purpose in analyzing multiple cases is to determine which case may be the most effective and applicable under varying system scenarios.

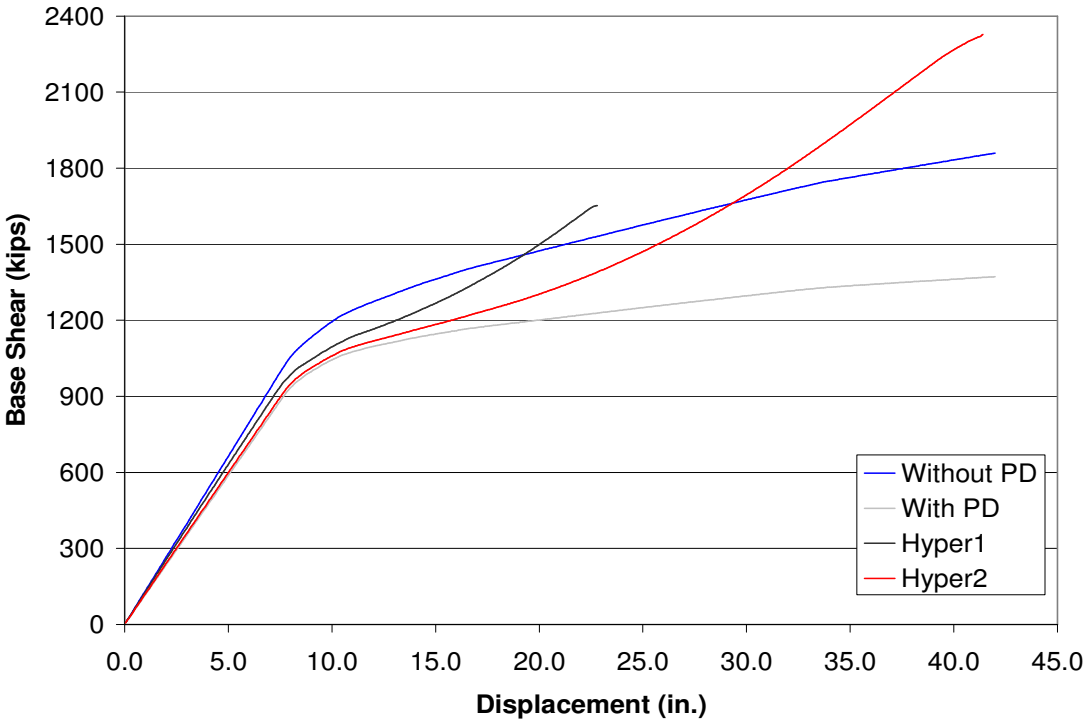

Figure 4.9 – Pushover Curves for P-Delta Case 1 with Hyperelastic Braces Installed

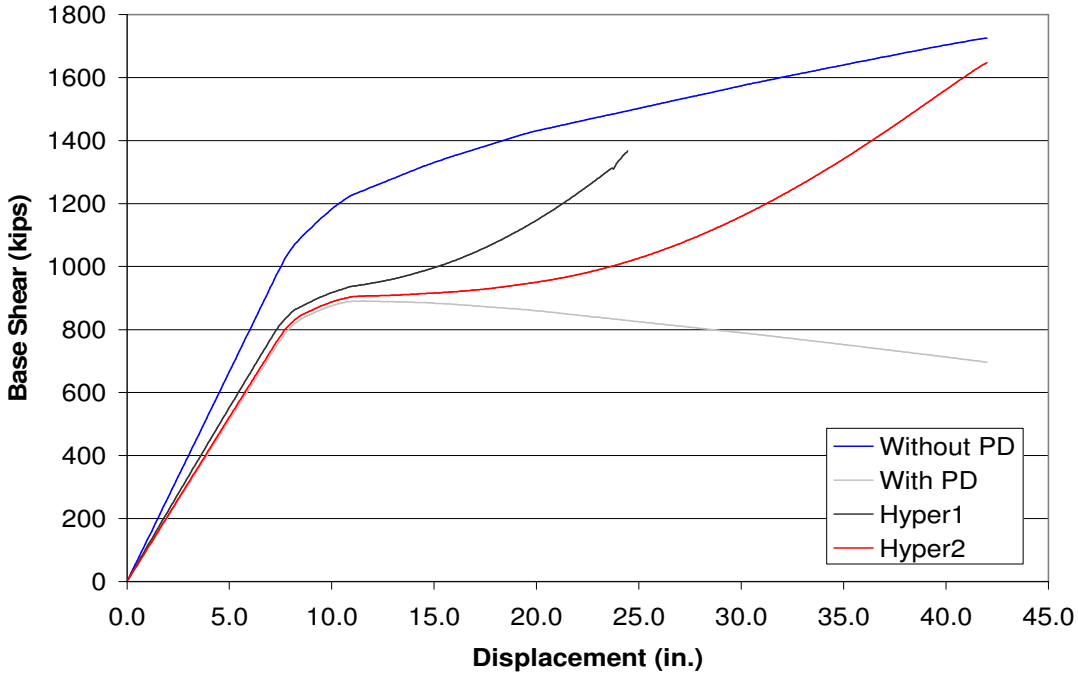

Figure 4.10 – Pushover Curve for P-Delta Case 2 with Hyperelastic Braces Installed

Once the pushover curves were established with the hyperelastic braces installed in the moment frame, verification on the equilibrium of system forces was performed using a nonlinear dynamic analysis of the frame. This analysis was completed to verify that the solution for the system satisfies equilibrium and is not converging on an erroneous solution. The system was checked to determine if the system forces calculated using Newton's law (F=ma) correlate to the measured system forces. The relative acceleration of each floor was used to calculate the base shear response history. This was compared to the measured column shears plus brace force response history, and the two plots give exactly the same results.

4.7 Analytical Procedures

The models established for the moment resisting frame are analyzed under a variety of analytical procedures to fully assess the performance characteristics of the hyperelastic braces. First, nonlinear static pushover analyses are performed, followed by nonlinear dynamic analysis of the frame under individual ground motions. Finally, incremental dynamic analysis is performed on the frame using incrementally scaled versions of the ground motions to assess the frame under a variety of ground motion intensities.

The initial assessment of the frame consists of nonlinear static pushover analyses. These analyses allow for the determinations of the hyperelastic brace properties, as well as the expected system post-yield behavior once the braces are installed. Nonlinear pushover analyses are performed for the system with and without both P-Delta cases, as well as with and without both sets of hyperelastic braces under each P-Delta case. The results from these analyses can be seen in Figures 4.7 through 4.10.

The next step in the analytical procedures is the nonlinear dynamic analysis of the moment frame. This procedure was performed under each of the P-Delta cases, with both sets of hyperelastic braces installed under each. Using two ground motions, this creates a total of 4 dynamic analysis cases per P-Delta case. These analyses are used to assess the unscaled dynamic performance of the frame with and without braces installed, for a total of 12 nonlinear dynamic analyses.

The two ground motions chosen for the nonlinear dynamic analyses and the incremental dynamic analyses are the El Centro ground motion (5/19/40, 04:39) and the Northridge ground motion (1/17/94, 04:31). The El Centro ground motion is a far field earthquake with significant high frequency content and relatively constant intensity across the record. The Northridge ground motion is a near-field earthquake that contains less high-frequency content and greater ranges of intensity across the record. The Northridge ground motion contains much more intensity than El Centro when the scales are compared. The duration of the Northridge ground motion is 14.95 seconds, while the duration of the El Centro ground motion is significantly longer at 40.0 seconds. The differences between the two ground motions should provide a sufficient range of response variability in the model while minimizing the scope of the analyses for the sake of simplicity. Figures 4.11 and 4.12 show the acceleration history for each ground motion. Figures 4.13 and 4.14 show the acceleration spectra for both ground motions for comparison.

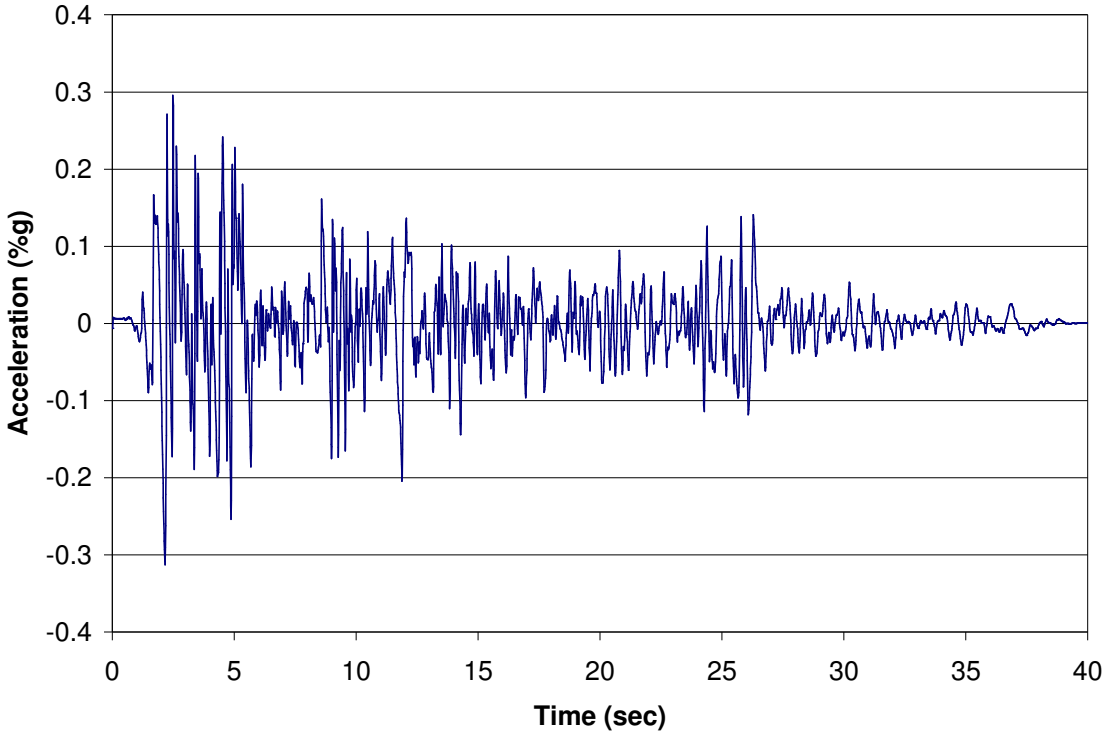

Figure 4.11 – El Centro Ground Motion Accelerogram

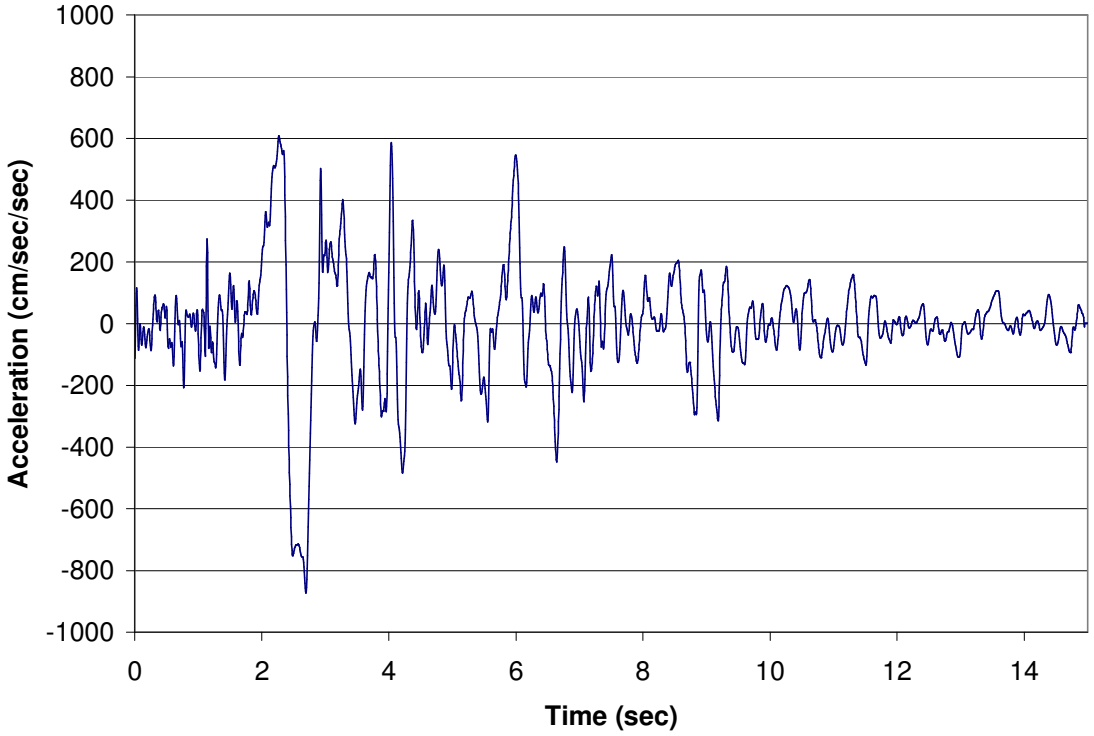

Figure 4.12 – Northridge Ground Motion Accelerogram

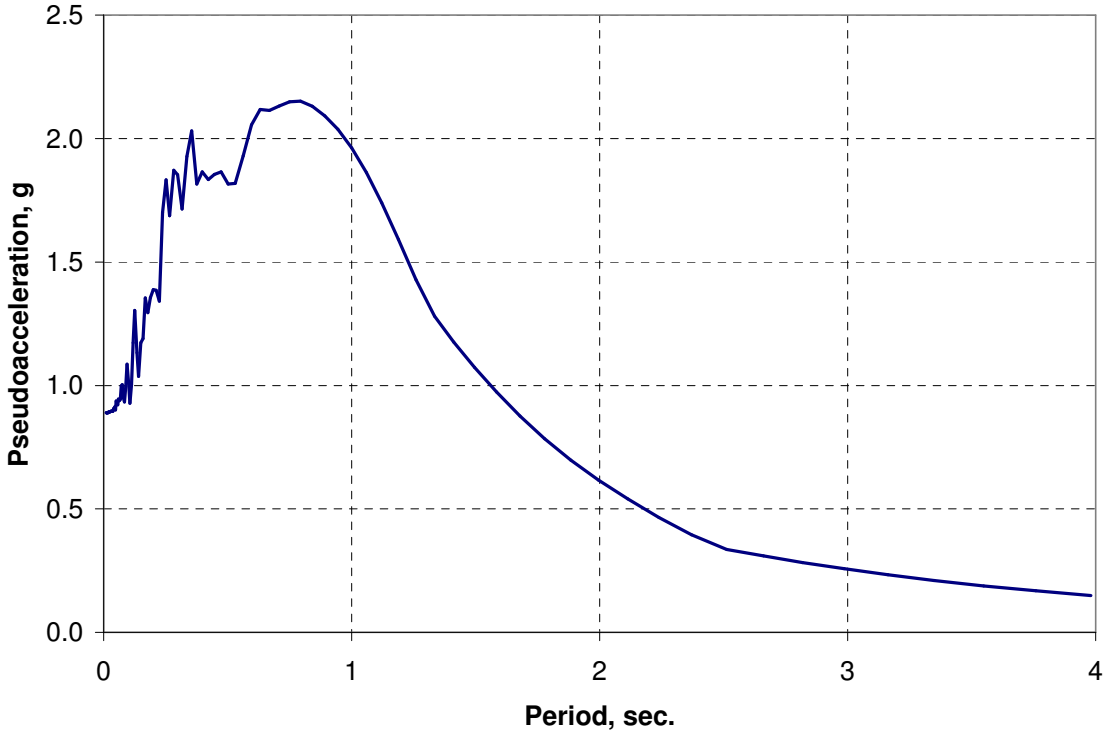

Figure 4.13 – El Centro Ground Motion Acceleration Spectrum

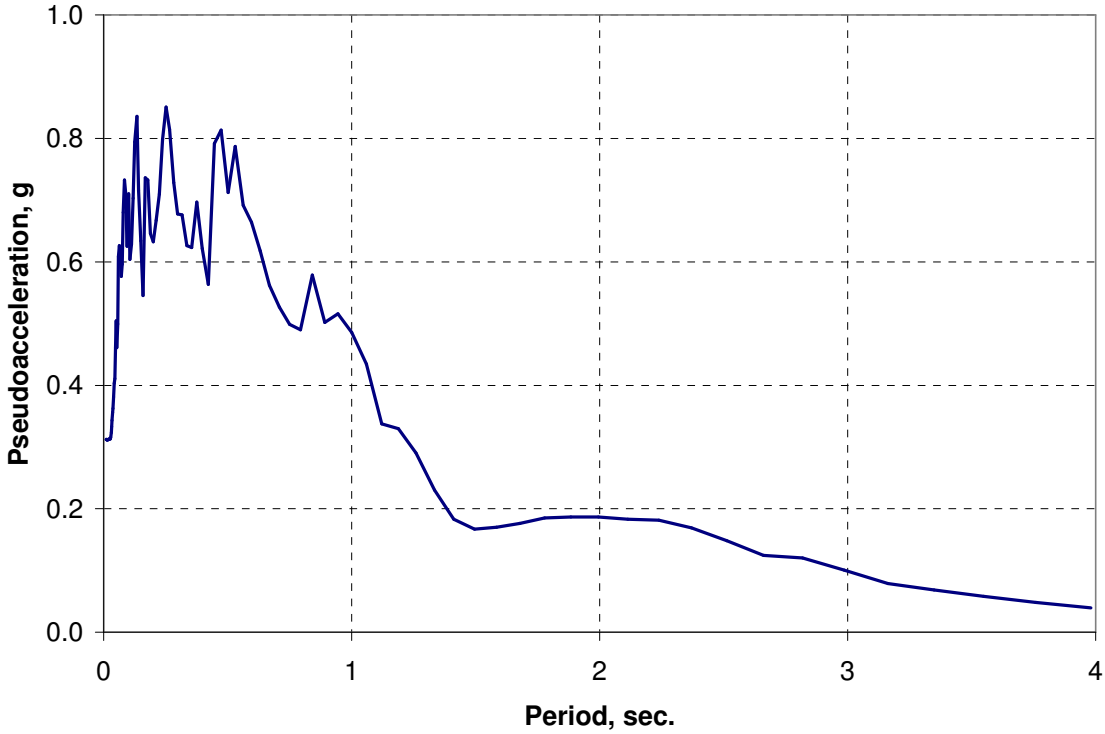

Figure 4.14 – Northridge Ground Motion Acceleration Spectrum

The final step in the analyses is to subject the moment resisting frame to incrementally scaled versions of the two ground motions ranging in intensity from 0.2 to 2.0. To reach the desired level of inelastic and unstable behavior, the El Centro ground motion is scaled up to 4.0 in some cases. The incremental dynamic analysis of the frame will measure the maximum interstory drift ratio for each story of the structure, as well as the maximum base shear of the system at each ground motion intensity. This will allow the creation of IDA curves to determine the effectiveness of each hyperelastic brace set under the different ground motion and P-Delta scenarios.

The IDA curves should demonstrate the effectiveness of the braces under a range of dynamic intensities. The brace influence is expected to be minimal on both drift and base shear at low intensity levels and most effective at the higher intensity levels. Also, the IDA curves should show which hyperelastic relation is effective in reducing the variability, therefore showing which ductility range is most effective for the hyperelastic equations for a MDOF structure. Both ground motions should provide sufficient

dispersion in the behavior of the frame to show that the hyperelastic braces reduce the response variability.

Chapter 5 - Results and Discussion

5.1 – Introduction and Overview of Results

The results for the analysis of the MDOF moment resisting frame are presented according to the order of the performed analyses. The results from the different modeling parameters are separated according to relevancy, and a discussion is provided regarding the important details for each section.

The first results focus on the responses obtained for the moment resisting frame from the baseline dynamic analyses. This set of analyses refers to the nonlinear dynamic analyses performed on the frame to obtain response history information. The frame is subjected to two different ground motions under two P-Delta scenarios. In each P-Delta case, two sets of hyperelastic equations are analyzed under both ground motions for their influence on interstory drift and base shear.

The hyperelastic equations will be referred to as Hyper 1 and Hyper 2 for the discussion of the results. Hyper 1 refers to the set of hyperelastic braces assigned to the response polynomials that gains greater stiffness at lower displacement levels. Hyper 2 refers to the set of hyperelastic braces assigned to the polynomials that stiffen over a greater displacement range. The results of the frames with hyperelastic devices are then compared to those obtained for the same frame with no hyperelastic bracing under the same P-Delta case and ground motion.

The results from the incremental dynamic analysis of the frame are discussed according to ground motion. Each ground motion is divided according to the P-Delta case under which it was analyzed, and then the effects produced by each hyperelastic equation set are discussed. The analyses are performed to investigate the influence of the hyperelastic braces on interstory drift ratio, maximum displacement, and system base shear. Like the dynamic results, each case is compared to an unbraced frame analysis under the same P-Delta effects.

5.2 – Baseline Dynamic Results

The baseline dynamic investigation consists of nonlinear dynamic analyses of each model setup for the moment resisting frame. The response histories are formed for the frame for the El Centro and Northridge ground motions under two P-Delta cases to assess the influence of two sets of hyperelastic braces.

The moment frame is first analyzed under the first P-Delta case for the El Centro ground motion and the Northridge ground motion. The decrease in system strength caused by the first case P-Delta effects is summarized in the pushover curve shown in Figure 4.5. The results for interstory drift and base shear are obtained for the frame with both sets of hyperelastic equations and for an unbraced frame without devices the results are then compared.

For both ground motions, the response histories show specific behavioral influences due to the hyperelastic braces under the first P-Delta case. Although low amounts of yielding occur in the frame under this P-Delta case, the braces are still influential in the frame behavior. The Hyper 1 braces create the most influence on both interstory drift and base shear due to the early stiffening behavior prescribed by the polynomials. The third and sixth stories are determined to be the controlling responses for drift in the moment frame, so the drift responses of those stories are used for the response histories and later for behavioral comparisons of drift under IDA. The unstable response of the system will be investigated under incremental dynamic analysis.

The interstory drift response histories are shown for the third story of the moment frame under both ground motions in Figures 5.1 and 5.2. These two graphs show the influence of both sets of hyperelastic devices on the response of the frame. Under the El Centro ground motion, the Hyper 1 braces create the most noticeable influence. When compared to the response of the frame without braces, the interstory drift is reduced during the first quarter of the response history, and then increased during the middle. This is due to a change in response phase caused by the amount of stiffness added by the Hyper 1 braces.

Over-stiffening is an effect instilled on the response of the structure due to the presence of the hyperelastic braces. The braces add force in opposition to the initial deflection in the structure, causing the observed reduction in drift. Then, as the

deflection of the structure changes quickly under the ground motion, the forces in the hyperelastic braces act in the direction of the displacement to increase the deflection of the system. This creates a rubber band-like effect due to the presence of the braces. An example of the increase in response due to over-stiffening can be seen at a time of 25 seconds in Figure 5.1. This response is also observed in the response under the Northridge ground motion. The over-stiffening response creates localized increases in interstory drift and base shear; however, the maximum values of response are not influenced by this brace effect.

Under the Northridge ground motion, the interstory drift ratios show more improvement due to the stiffening of the hyperelastic braces as shown in Figure 5.2. Both braces stiffen during the initial pulse from the ground motion where drifts are shown to decrease. Upon the subsequent reversal of deflection from the ground motion, the resistance of the braces in the direction of the initial deflection causes an increase in drift ratio due to over-stiffening. Essentially, the braces fling the structure back in the opposite direction when the deflection of the structure is suddenly reversed. This is visible in Figure 5.2 at second 3.

The response of the plain frame shows an acquired amount residual drift at the end of the response history. The Hyper 2 braces cause an up-shift in the direction of the drift ratios, and result in very little residual displacement at the end of the response history. The Hyper 1 braces contribute too much stiffness and cause the frame to acquire an amount of residual displacement opposite in direction than the unbraced frame at the end of the response history. However, the residual displacement is still less than the amount acquired by the plain frame. This behavior highlights the stabilizing behavior of the hyperelastic devices

The base shear response histories are summarized for these analyses in Figures 5.3 and 5.4. The base shear response of the frame increases in relation to the resistance to interstory drift. Under the El Centro ground motion, the frame experiences an increase in system forces during the high intensity portion of the ground motion due to both sets of hyperelastic braces. This is due to the stiffening response of the braces, which reduces the drift of the frame over this segment of the response.

The base shear is shown to increase for the frame with Hyper 1 braces during the middle of the response history due to the increase of displacement that occurs. The

Hyper 2 frame shows significant increase in base shear only over the first 5 seconds of the response where deflections are the highest; the increase over the rest of the response is very small.

Under the Northridge ground motion, the base shear is shown to increase most noticeably during the first 4 seconds of response. Both sets of braces cause a significant increase in the base shear during the large pulse that occurs over this time frame, as shown in the response history in Figure 5.4. Each brace set increases the base shear in proportion to the reduction in drift they cause. Unlike the response to El Centro, the braces have little effect on the magnitude of base shear during the last half of the response history. The main response of the structure occurs during the pulse between 2 and 4 seconds, and the braces show their effectiveness during this section. After the main demand of the ground motion is past, only the residual drift remains and the system forces are not greatly influenced. This highlights the demand based performance of the braces.

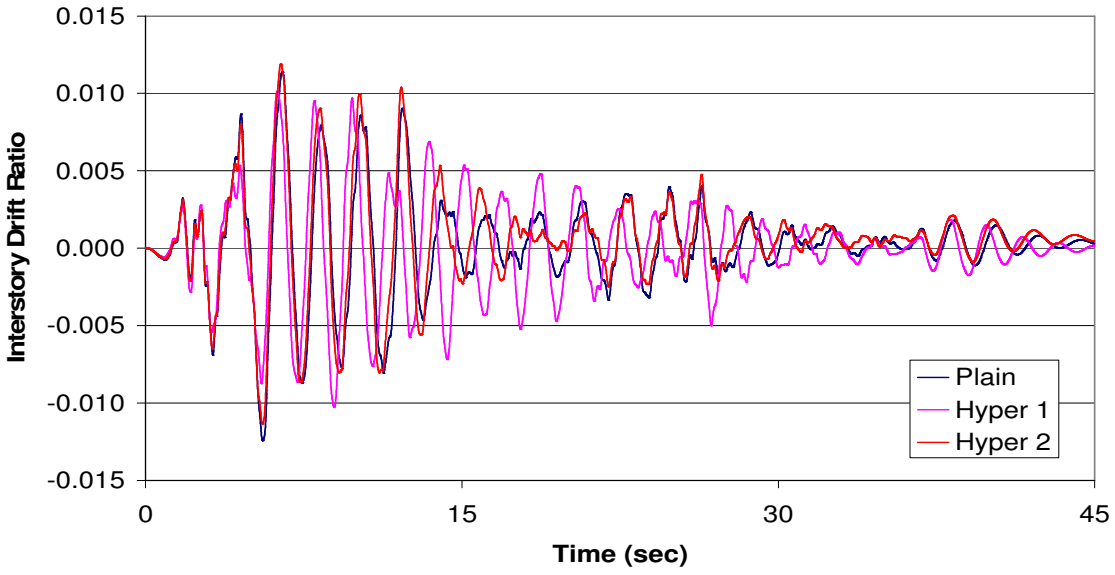

Figure 5.1 - Third Story Interstory Drift Ratio Response History, El Centro P-Delta Case 1

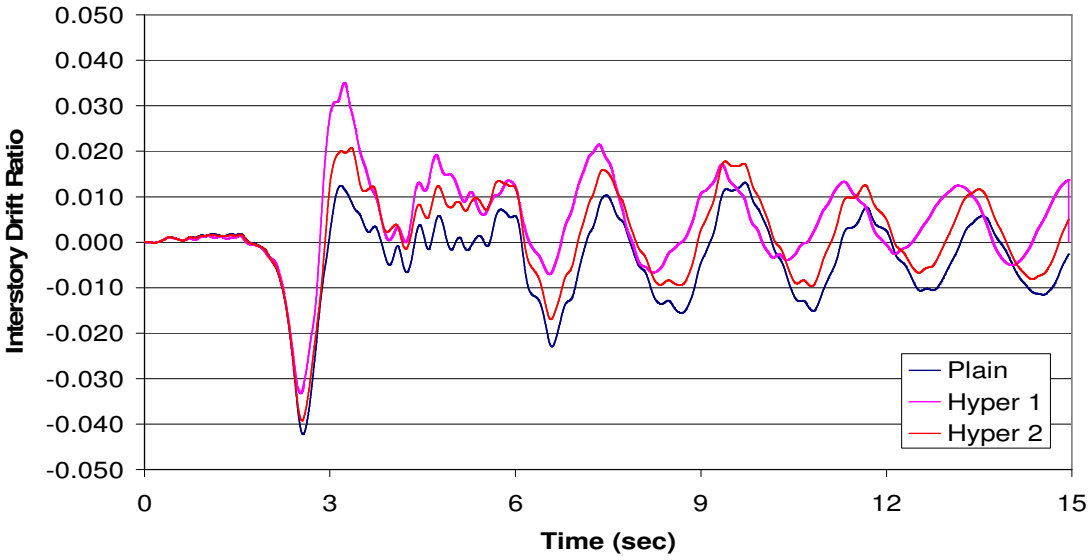

Figure 5.2 - Third Story Interstory Drift Ratio Response History, Northridge P-Delta Case 1

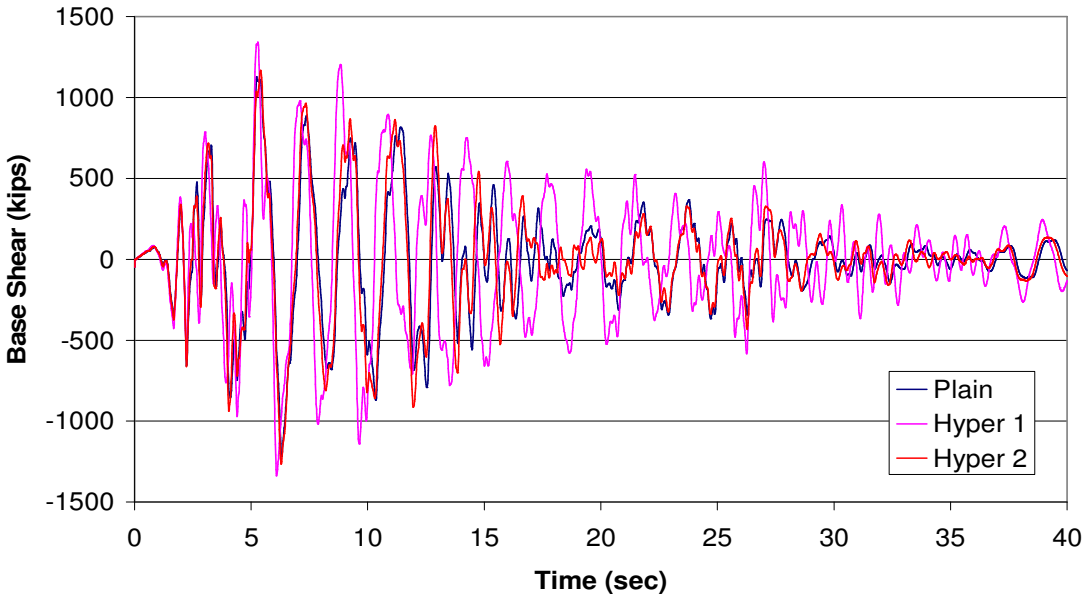

Figure 5.3 - Base Shear Response History for El Centro P-Delta Case 1

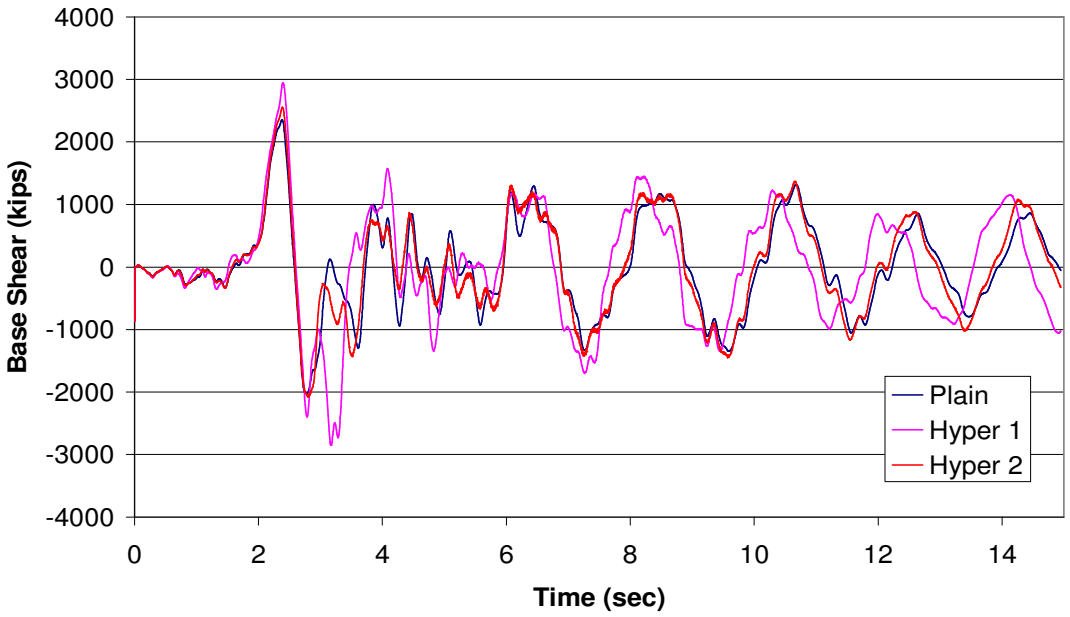

Figure 5.4 - Base Shear Response History for Northridge P-Delta Case 1

More distinct differences in the behavior of the frame are visible in the results from the dynamic analyses of the second P-Delta cases. The same nonlinear dynamic analyses were performed for both ground motions and both sets of hyperelastic braces under the more severe second case of P-Delta effects. This set of P-Delta effects is expected to cause more nonlinear and unstable responses in the structure. The decrease in system strength due to the second case P-Delta effects are summarized in the pushover curve shown in Figure 4.6.

The response histories show more yielding behavior under the second P-Delta case through residual displacements. This is due to the negative secondary stiffness present in the system after yielding. The drift ratio response histories may be found in Figures 5.5 and 5.6 for the El Centro and Northridge ground motions, respectively. The Northridge ground motion causes the most yielding and thus creates the best scenario for evaluating the performance of the hyperelastic braces for peak and residual drift. As more yielding occurs, the braces become more influential and thus have a greater impact on the response of the structure.

Under the El Centro ground motion, a similar pattern of response is observed as shown for the first P-Delta Case. The drift ratios of the plain frame are larger, and the frame acquires residual drift at the end of the response. Both sets of hyperelastic braces respond to provide more noticeable reduction in displacement in the frame.

The Hyper 2 braces demonstrate a small amount of increased drift during the first 15 seconds of the response due to over-stiffening as mentioned under the first P-Delta case. This effect is small and occurs in the direction of positive drift. These braces also decrease the residual displacement of the structure and reduce the peak drift values displayed in the plain frame. The Hyper 1 braces increase the magnitude of the positive-sign drift in the frame. The increase in positive drift occurs as the stiffening of the braces shifts the entire response of the interstory drift upwards. While some of the increased magnitude of positive drift may be due to over stiffening of the braces, the net effect of the stiffer braces is desirable due to the larger extent of yielding in the structure and the residual displacement that is acquired. The absolute average of peak interstory drift does not increase, the peak values of drift are decreased, and the braces eliminate residual displacement in the response.

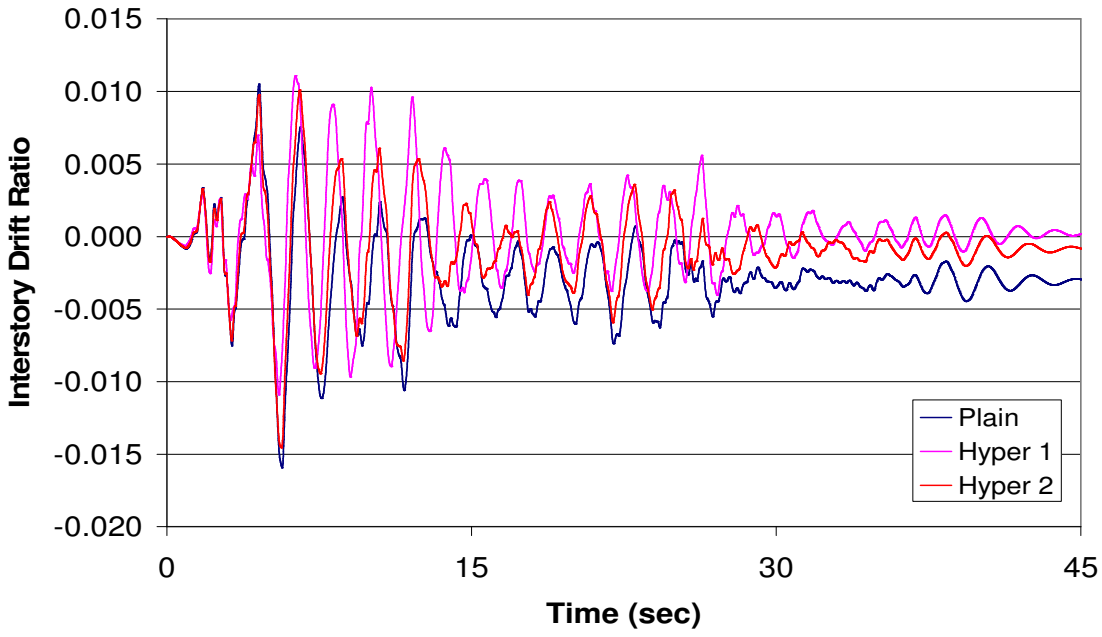

Figure 5.5 - Third Story Interstory Drift Ratio Response History, El Centro P-Delta Case 2

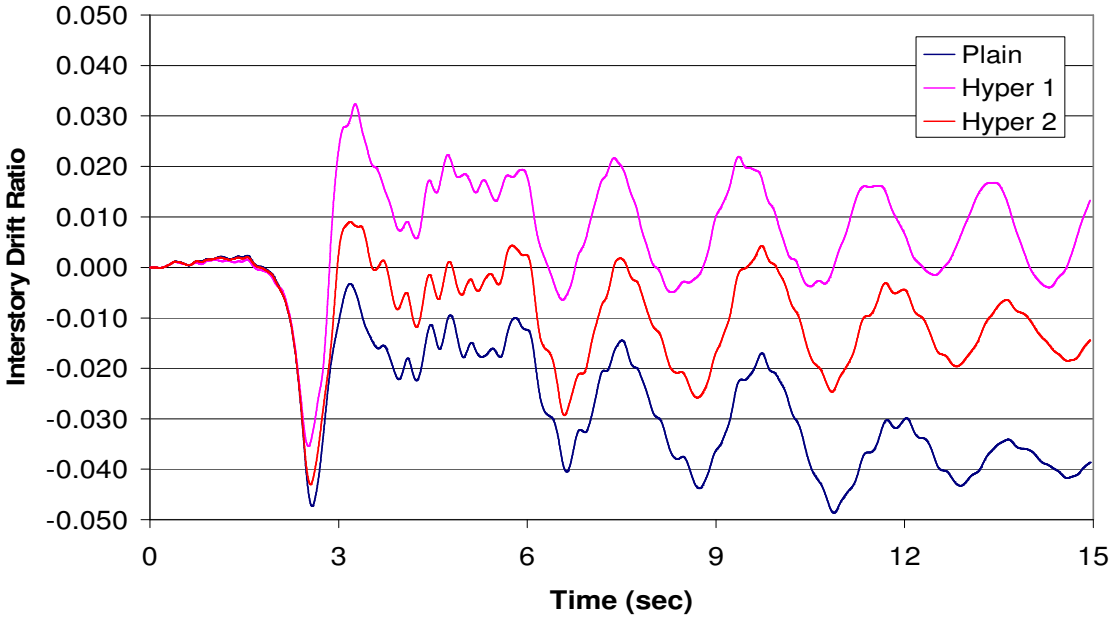

Figure 5.6 - Third Story Interstory Drift Ratio Response History Northridge P-Delta Case 2

Figure 5.6 shows the response histories for interstory drift under the second case P-Delta effects. Both sets of braces are shown to greatly increase the structural response under this load case. The unbraced frame is shown to acquire large peak interstory drift values, as well as significant residual drift. Both sets of braces greatly reduce both the peak drift values, as well as the residual drift values. Again, the Hyper 1 braces provide too much stiffness and result in a reversal of residual displacement, but only slightly. The over-stiffening response is again noticed during the large pulse in the ground motion, however this response by the braces is used to reduce the residual drift. This response history highlights the stabilizing potential for the hyperelastic brace sets.

The base shear response histories for the second P-Delta case are given in Figures 5.7 and 5.8. Under the El Centro ground motion, the frame with the Hyper 2 braces displays the smallest increase in base shear in accordance with the reduction in drift these braces create versus the plain frame. The forces increase most significantly during the first 5 seconds of the response where the drift is reduced the most. The Hyper 1 braces create a positive effect in terms of drift; however, the base shear is increased significantly as a result. The peak base shear values increase as much as 20%, and there is a significant increase in base shear response during the second half of the response history.

The increase in base shear is due to another over-stiffening response from a pulse that occurs in the system at 27 seconds, and due to the response of the braces against the already accumulated residual displacement in the plain frame.

Under the Northridge ground motion, the base shear response history is very similar to the response produced for the first P-Delta case. Both braces increase the system forces significantly during the initial pulse of the ground motion, and the remainder of the response history does not vary greatly between the bracing schemes. The Hyper 1 braces create the most increase in base shear due to their earlier stiffening behavior, and the only significant increase in base shear due to the Hyper 2 braces is during the first 4 seconds of the response history. Only one base shear pulse is significantly increased, and the overall damage is reduced in the systems due to reduced residual drifts.

The magnitude of the base shear experienced by the frame under the second P-Delta case seems to contradict the system capacity shown in the pushover curve in Figure. 4.6. However, the increased capacity occurs due to inconsistencies between dynamic analysis and static pushover analysis. The pushover analysis capacity is proportional to an evenly distributed lateral load pattern that is not equivalent to the lateral loading produced during the used ground motions. Therefore, increased system capacities are possible beyond the pushover curve values.

The computed behavior of the frames with hyperelastic braces subjected to two different ground motions clearly illustrates the stabilizing potential of the braces. The response of interstory drift in the frame may be usefully compared to the related base shear response to show the efficiency of the braces. The residual drifts observed in the responses of the unbraced frames are reduced in all cases; however the increase in system forces may partially negate the positive drift response contributed by the braces.

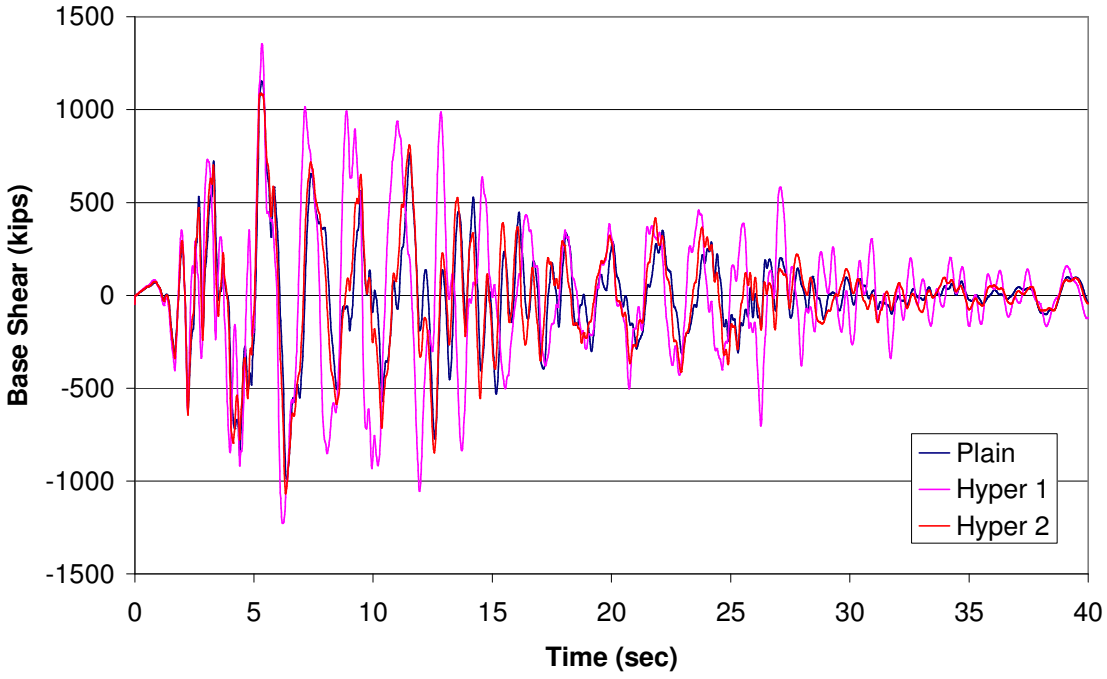

Figure 5.7 - Base Shear Response History for El Centro P-Delta Case 2

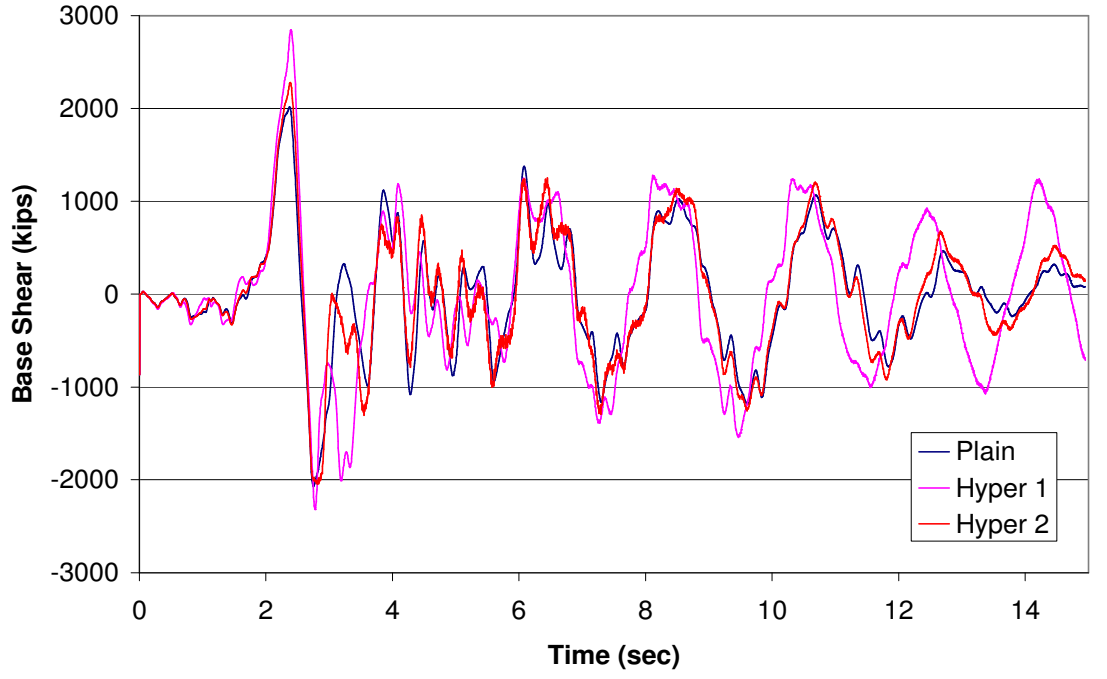

Figure 5.8 - Base Shear Response History for Northridge P-Delta Case 2

From the two sets of baseline dynamic analyses performed on the structure, the important response measures can be noted for future observation under the process of incremental dynamic analysis. The most important characteristics include the point in the system response at which the hyperelastic braces begin to influence the behavior, and the amount of residual displacement acquired by the unbraced structure. Also important is how each set of braces influences system forces relative to the system displacement. These measures are important behavioral benchmarks in determining the effectiveness of hyperelastic braces using IDA.

The observations for both ground motions show that under these unscaled levels of ground motions with distinctly different characteristics, the hyperelastic braces are influential in more areas of response than the deflection ranges for which equations are designed. The over stiffening response of both braces can be seen to cause increased drift and base shear in areas of the response history, and it's influence may be further analyzed under incremental dynamic analysis. The dynamic characteristics of the frame and the ground motion combine to create a complex response from the frames, and the process of incremental dynamic analysis may shed more light on this behavior.

5.3 – Incremental Dynamic Analysis Results – El Centro

The incremental dynamic analysis of the moment resisting frame consists of multiple full-scale nonlinear dynamic analyses under a scaled ground motion during which specific maximum response measures are recorded. Like the baseline dynamic analyses, the moment frame is analyzed under both P-Delta cases for both ground motions to investigate the behavior of the two sets of hyperelastic equations. The results will be presented based on ground motion, focusing on each response measure and how the frame behavior is influenced by the varying hyperelastic braces and P-Delta cases.

Under the El Centro ground motion, the incremental dynamic analysis is performed to investigate base shear and interstory drift response measures. The IDA curves for the unbraced frame demonstrate the largest amount of variance in the IDA curves, along with the greatest magnitudes of the response measures. The response shows that as responsiveness of the hyperelastic brace increases in the system, the amount of variance decreases and the magnitude of drift decreases at all levels. The

regularity of the curves refers to the predictability and variability present in the path they follow.

The first P-Delta case is most positively influenced under IDA by the Hyper 1 set of braces in terms of interstory drift magnitude and curve regularity. The next three figures show the interstory drift IDA curves for each level of the moment frame under the El Centro ground motion and the first P-Delta case. Figure 5.9 shows the IDA curves for the plain frame, Figure 5.10 shows the curves for the frame with the Hyper 2 braces installed, and Figure 5.11 shows the curves for the frame with the Hyper 1 braces installed. On the ordinate, pga denotes peak ground acceleration. The curves are displayed in the order of increasing hyperelastic behavior at lower displacement increments. The Hyper 2 braces display the most gradual stiffening, and therefore provide the first increment of hyperelastic influence on the system.

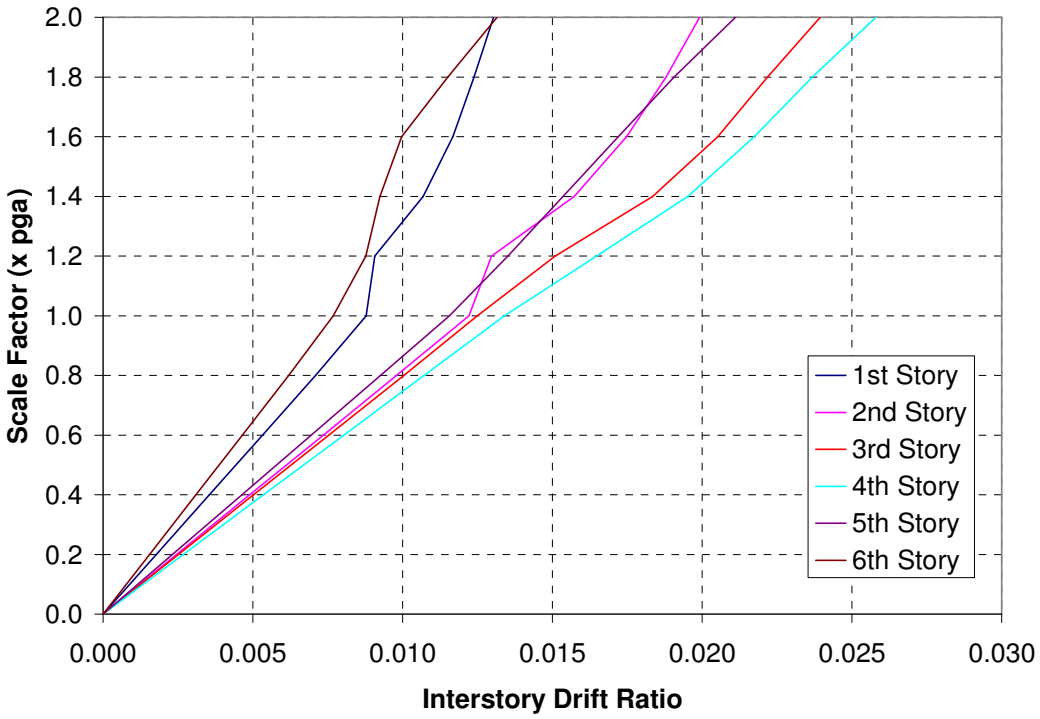

Figure 5.9 - Story Drift Ratio IDA Curves El Centro, PD 1, Plain Frame

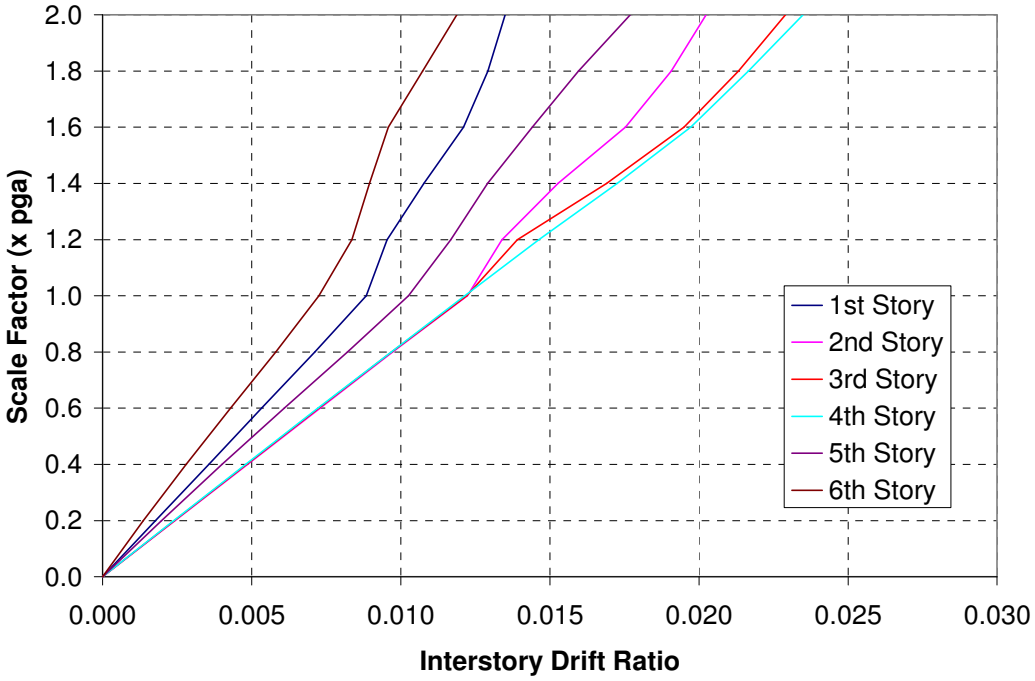

Figure 5.10 - Story Drift Ratio IDA Curves El Centro, PD 1, Hyper 2

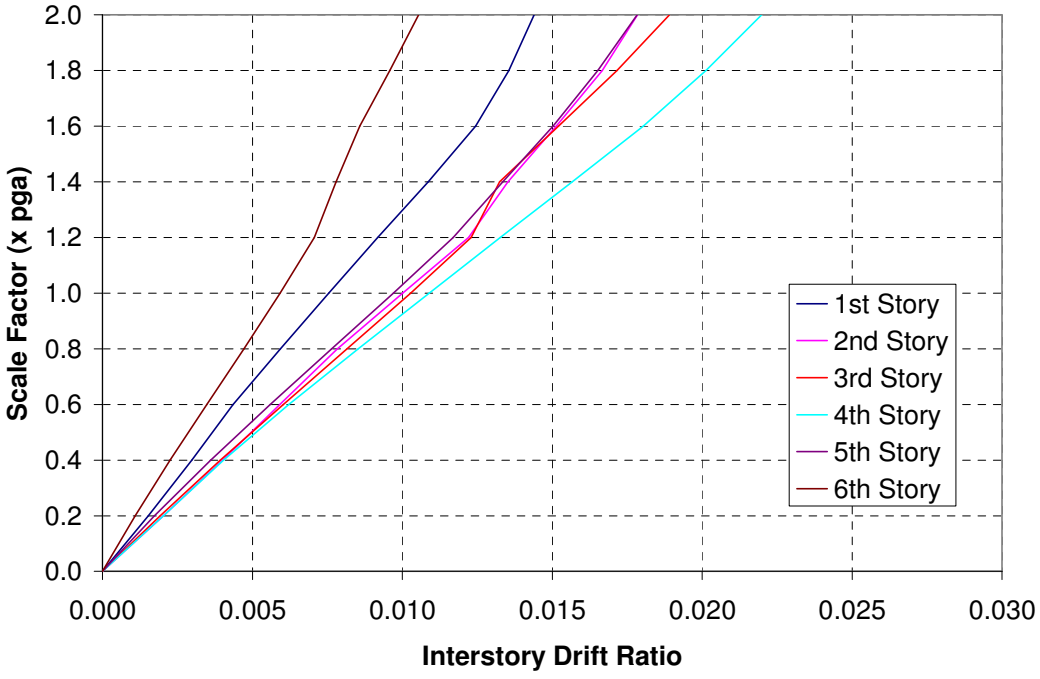

Figure 5.11 - Story Drift Ratio IDA Curves El Centro, PD 1, Hyper 1

The trends in the graphs show the influence of the braces on the pattern and magnitude of the IDA curves. The interstory drift ratios of each level follow a more predictable and less variant path as the hyperelastic responsiveness increases. The plain frame exhibits significant amounts of irregularity in the curves for each story. This translates to a lack of predictability in overall dynamic performance. The Hyper 2 braces begin to reduce the amount of variability present in the curves, and the Hyper 1 braces create a more predictable curve set.

The magnitude of interstory drift is reduced as hyperelastic brace responsiveness increases. The Hyper 2 equations reduce the magnitude of the drift ratios by an average of 2 percent per floor at the largest scale factor. The Hyper 1 equations further reduce the magnitude of the interstory drift ratios by another 1 percent. Along with the increased curve regularity, the Hyper 1 braces show the most positive influence on the drift behavior of the moment frame under the first P-Delta case IDA. This drift behavior will be compared to the related base shear behavior to see the efficiency of the braces in reducing drift while limiting the increase of system forces.

Since the first P-Delta case never acquires a negative secondary strength, the system remains capable of gaining load under a theoretically infinite increasing displacement. Therefore, instability may never occur under this scenario. However, the capacity remains permanently reduced beyond yield and thereby benefited by the presence of the braces in terms of deflection. For the second P-Delta case, the scaling is increased to 4.0 to attempt to further investigate the behavior of the systems beyond yield.

A yielded system in a base shear IDA analysis behaves opposite to the graph of the pushover behavior. The IDA curves that steepen sooner indicate a weaker system that is quicker to loose load carrying capacity. As the IDA curve becomes steeper, the system experiences more yielding and loss of strength. A vertical line theoretically indicates a complete loss of strength. Curves that bend farther to the right indicate systems with more load carrying capacity and with larger values of acquired base shear.

The base shear IDA curves for first P-Delta case under the El Centro ground motion presented in Figure 5.12 show that the Hyper 1 braces result in the greatest increase in base shear. The graph shows that the system forces increase along a linear pattern until the yield point of the system is reached, after which the frames begin to lose

capacity in relation to the braces installed in each. While the Hyper 1 braces increase system forces the greatest, they also increase the load capacity of the system. The curve extends farther to the right and increases in slope at a lesser rate than the plain frame and the frame with Hyper 2 braces. Since the Hyper 1 braces provide the most stiffness to the system over the experienced range of deflection, these braces provide the greatest increase in base shear over the range of scaled ground motion.

The base shear of the moment frame is shown to not be significantly influenced by the presence of the Hyper 2 braces. In fact, as the intensity increases, the system is shown to experience less base shear with the Hyper 2 braces installed. This response can be attributed to the low amounts of stiffness the Hyper 2 braces contribute over the range of ductility demand provided by the system for this set of IDA.

The base shear curves for the El Centro ground motion show that both sets of braces contribute no increase in base shear before yielding occurs. This shows that the design objective of increased stability along with minimal increases in system forces under lower ground motion intensities is achieved by both sets of hyperelastic elements.

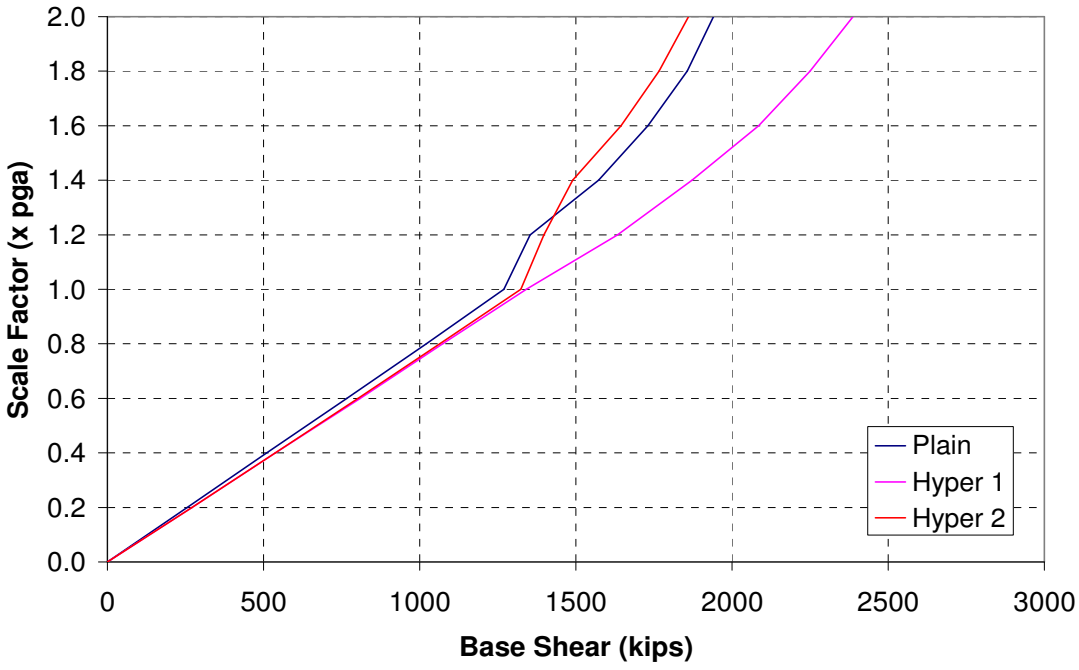

Figure 5.12 - Base Shear IDA Curves for P-Delta Case 1 El Centro

For the second P-Delta case under the El Centro ground motion, similar trends are found for both interstory drift and base shear. The drift response changes due to a larger amount of yielding that occurs in the earlier portion of system behavior, and due to the increased scaling of the ground motion. While some of the response trends change the maximum scaled ground motion, the increased scale means that these trends do not invalidate those observed for the first P-Delta case. The analyses were scaled up to 4.0 for this case to exaggerate the yielded system responses and the related increase in the influence of the hyperelastic braces.

The IDA curves the interstory drift ratio for the second P-Delta case effects under the El Centro ground motion can be found in Figures 5.13-5.15. The IDA curves for interstory drift again display less variability as more responsive hyperelastic elements are installed. The Hyper 1 brace set shows the greatest reduction in curve variability and response magnitude. The variability of the interstory drift ratios highlights the predictability of the system and how prone it may be to dispersion.

The interstory drift ratios for the plain frame are shown to improve for the majority of the levels when the hyperelastic elements are added; however, the responses for the 4^{th} and 5^{th} floors appear to worsen. A greater magnitude drift ratio is seen for this floor when both sets of braces are added versus the response of the unbraced frame. This curve behavior is due to irregularity in the system behavior at high ground motion intensity. The increase in drift is not due to any system parameters of concern, rather due to the decrease in variability of the response of the structure. As the regularity increases, this behavior is eliminated and the magnitude of the drift decreases at all other floors.

Base shear under the second P-Delta case for the El Centro ground motion again follows the same pattern as the first P-Delta case even though more yielding occurs in the system. This response can be seen in Figure 5.16. Due to the increase in scaling, the slope of the curves is not on the same scale as the previous IDA curves; however the Hyper 1 braces still show the most increase in system forces and system capacity. The Hyper 1 braces show a more significant addition to system forces earlier in the IDA curves due to the earlier point at which yielding occurs under this P-Delta case, and due to the increased scale of the graph.

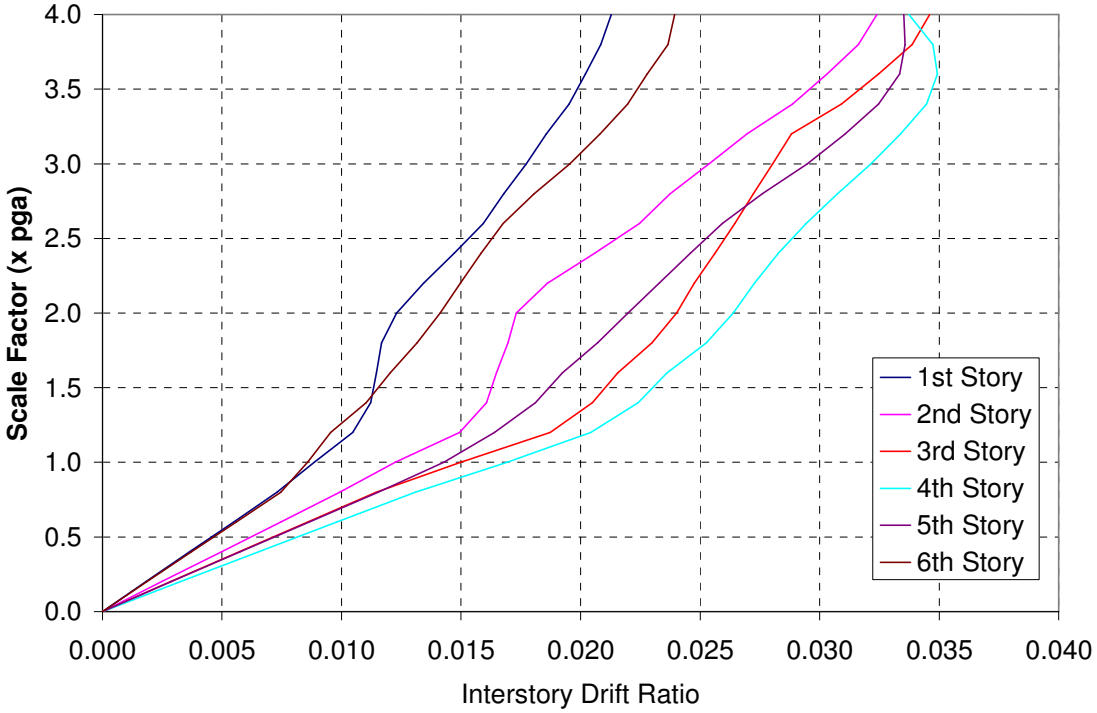

Figure 5.13 - Interstory Drift Ratio IDA Curves El Centro, PD 2, Plain Frame

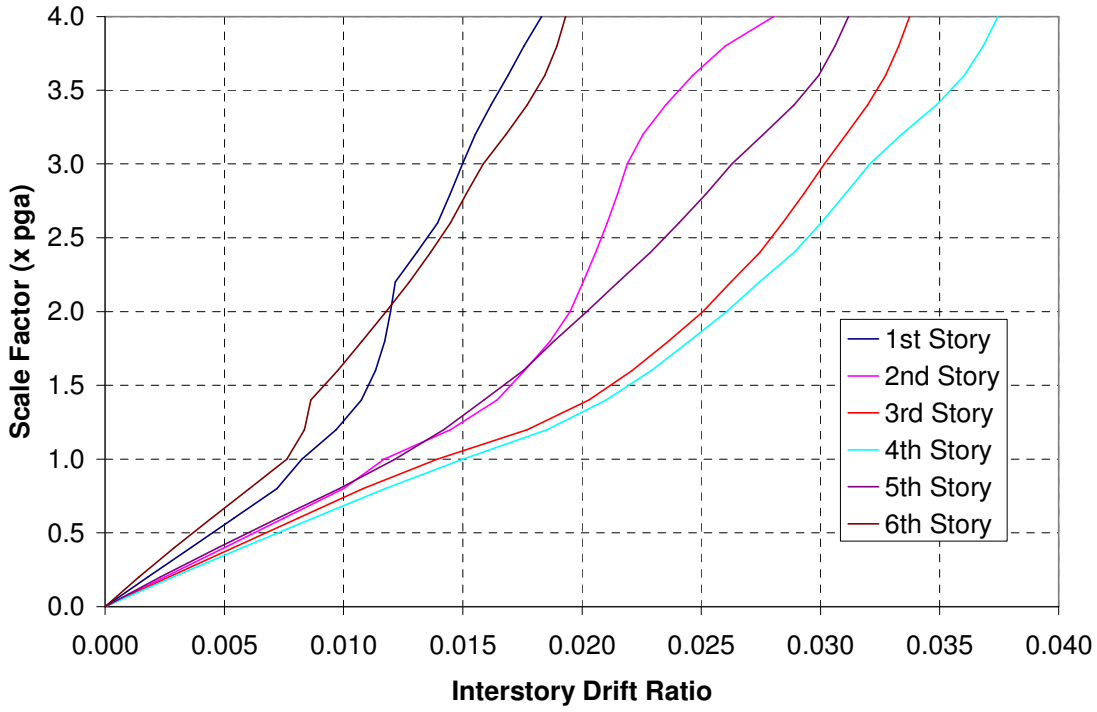

Figure 5.14 - Story Drift Ratio IDA Curve El Centro, PD 2, Hyper 2

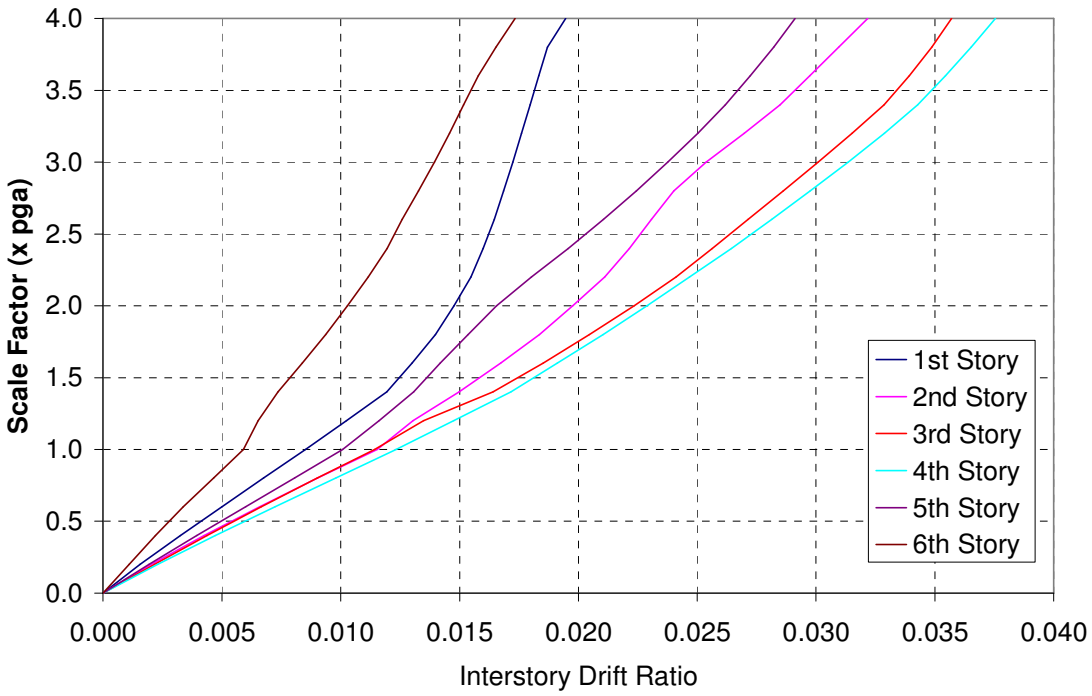

Figure 5.15 - Story Drift Ratio IDA Curves El Centro, PD 2, Hyper 1

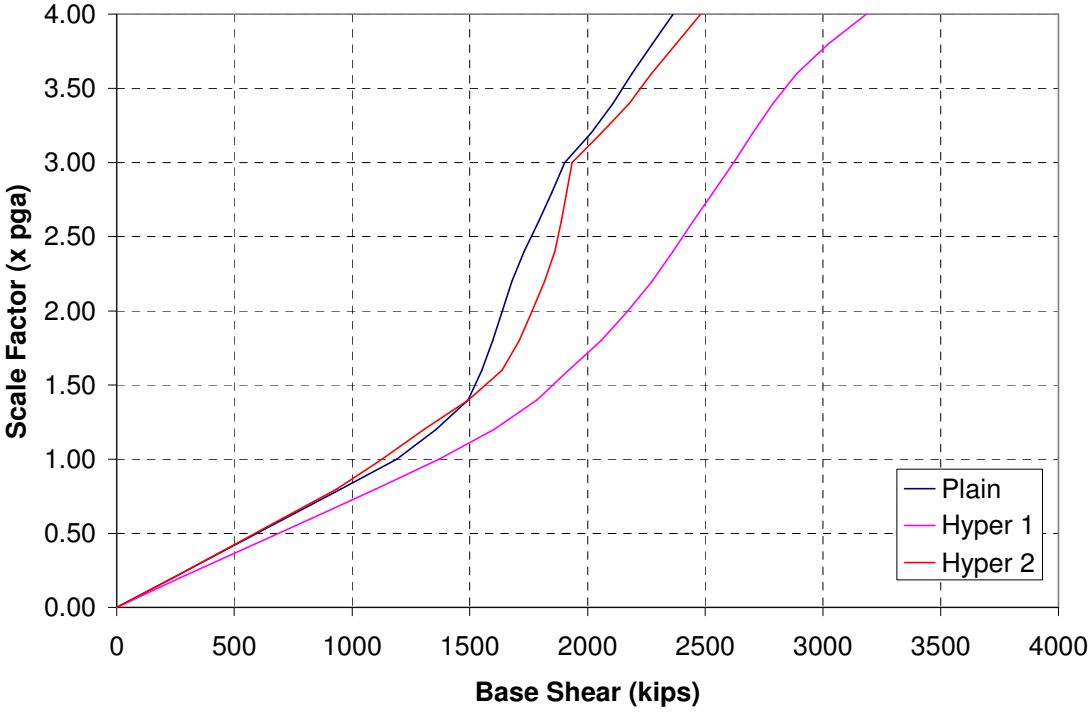

Figure 5.16 - Base Shear IDA Curves for P-Delta Case 2, El Centro

The Hyper 2 braces again exhibit only a small increase in system forces over the range of demand created by this IDA analysis. The braces do provide an increase in system predictability, however the magnitude of the drift responses are not improved as much as under the Hyper 1 braces. Although the scale of the analysis was doubled versus the first P-Delta IDA, the most efficient range of ductility required by the Hyper 2 functions may not be provided yet by the response of the frame.

The incremental dynamic analysis of the moment resisting frame provides further insight on the performance characteristics of the hyperelastic braces. The braces are shown to decrease curve variability and thus decrease the amount of dispersion expected in the results under multiple ground motions. The braces also demonstrate their stabilizing potential through the increased reduction of interstory drift.

5.4 – Incremental Dynamic Analysis Results - Northridge

The next set of incremental dynamic analysis to be performed on the moment frame involves the use of the Northridge ground motion under the first P-Delta case. Unlike the El Centro ground motion, an unstable response is achieved in this set of analyses. The new characteristics of the near field ground motion provide a basis for analyzing the stabilizing effects of the hyperelastic braces under an unstable system response.

For the first P-Delta case, the IDA curves for interstory drift show improved system performance towards the Hyper 2 set of equations. Figure 5.17 provides a comparison of interstory drift ratios for the sixth story of the structure between each hyperelastic bracing setup. The unstable drift response is visible in the curve for the plain frame. Only the summary of the IDA curves for the sixth story are shown for these analyses for the sake of comparing the responses of the braced frames on the same plot. The IDA curves for all of the stories may be found in Appendix D for reference.

As the system progresses into the range of ductility demanded by the Northridge ground motion, the Hyper 2 braces best match the requirement of the system. Both sets of hyperelastic braces show increased system performance; however, the Hyper 2 braces best match the ductility demand of the system and show the most efficient increase in

system performance. The Hyper 1 braces gain more stiffness under lesser drifts than the Hyper 2 braces and contribute much more stiffness when full displacements are experienced.

Figure 5.18 shows the base shear for the frame under the Northridge ground motion under the first case P-Delta effects. The Hyper 2 braces are shown to create the least increase in system forces between the brace types, and the increase in system forces is shown to be minimal at lower intensity levels for both sets of hyperelastic braces. The Hyper 2 braces provide nearly the same amount of drift protection at increasing scale factors for this ground motion while contributing significantly less base shear. This is due to the designed ductility range for the two sets of braces. The Hyper 1 set is designed to provide more stiffness at lower amounts of drift, therefore causing it to contribute increasing amounts of base shear as ductility demand increases beyond the designed range of effectiveness. The amount of base shear contributed by the Hyper 1 braces is entirely too high for acceptability beyond a scale factor of 1.2.

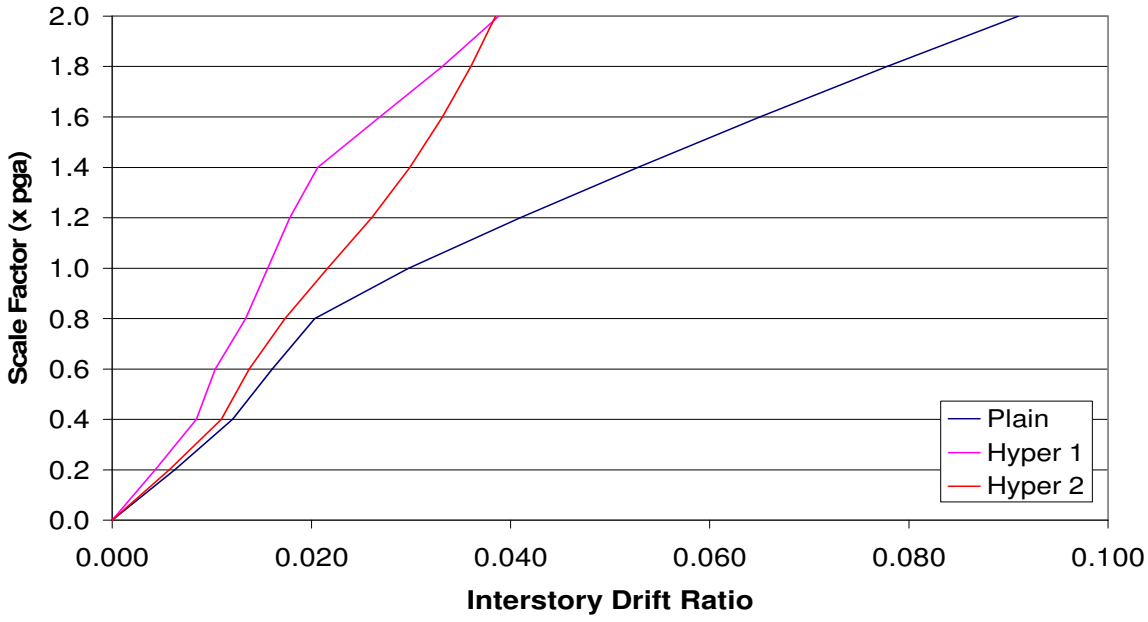

Figure 5.17 - Interstory Drift IDA Curve Summary for P-Delta Case 1 Northridge (sixth story)

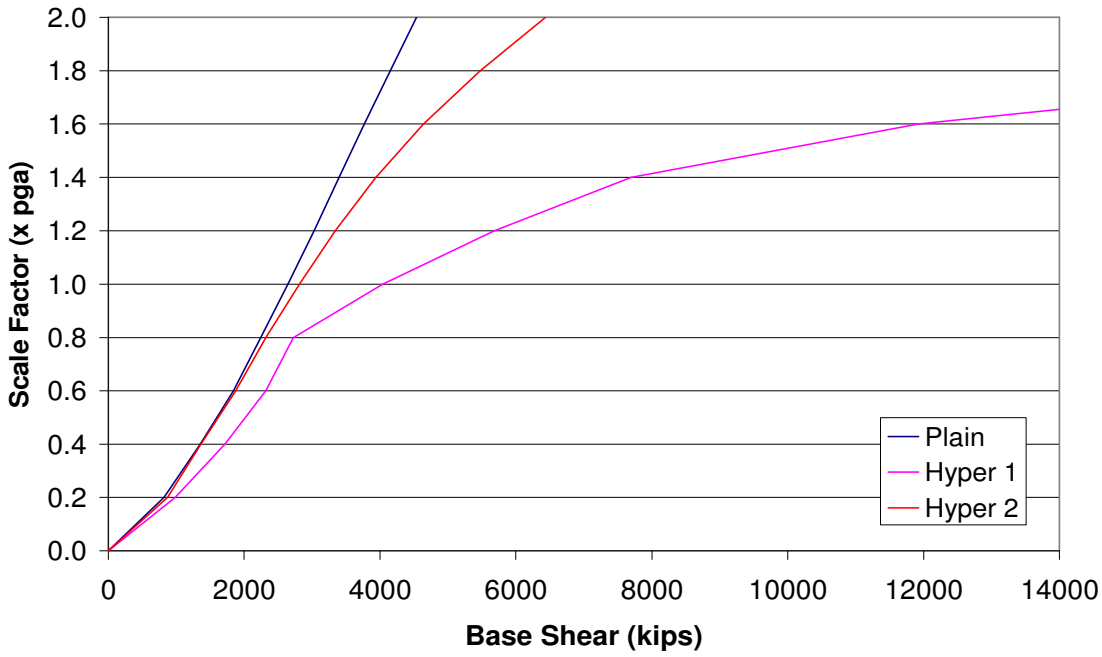

Figure 5.18- Base Shear IDA Curves for P-Delta Case 1, Northridge

The final set of incremental dynamic analyses performed on the moment frame involved the Northridge ground motion under the second P-Delta case. Like the first P-Delta case, the system experiences an unstable response in this set of analyses. This provides a second set of analyses to reinforce the stabilizing effects of the hyperelastic braces.

These IDA curves for interstory drift ratio and base shear may be found in Figures 5.19 and 5.20, respectively. The results for interstory drift ratio and base shear in these figures are the same as shown in the first P-Delta case. Both P-Delta cases cause instability in the system under this ground motion, with the only difference being the time at which this instability occurs in the system. The instability in the drift ratio IDA curves of the plain frame occurs at a lesser magnitude under the second P-Delta case. The two responses provided by the frame with hyperelastic braces are nearly identical between the two P-Delta cases, indicating a reliable stabilizing response under varying system parameters.

The trends again show that both sets of hyperelastic braces are effective in limiting the interstory drift at high ground motion intensities, with the Hyper 2 set being

the most effective. The base shear is shown to increase greatly under the Hyper 1 set as ground motion intensity increases, while the increase due to the Hyper 2 set is much less. This may be attributed to the ductility range over which the Hyper 2 set is designed to function, and shows that the Hyper 2 set is the most effective bracing set for the Northridge ground motion.

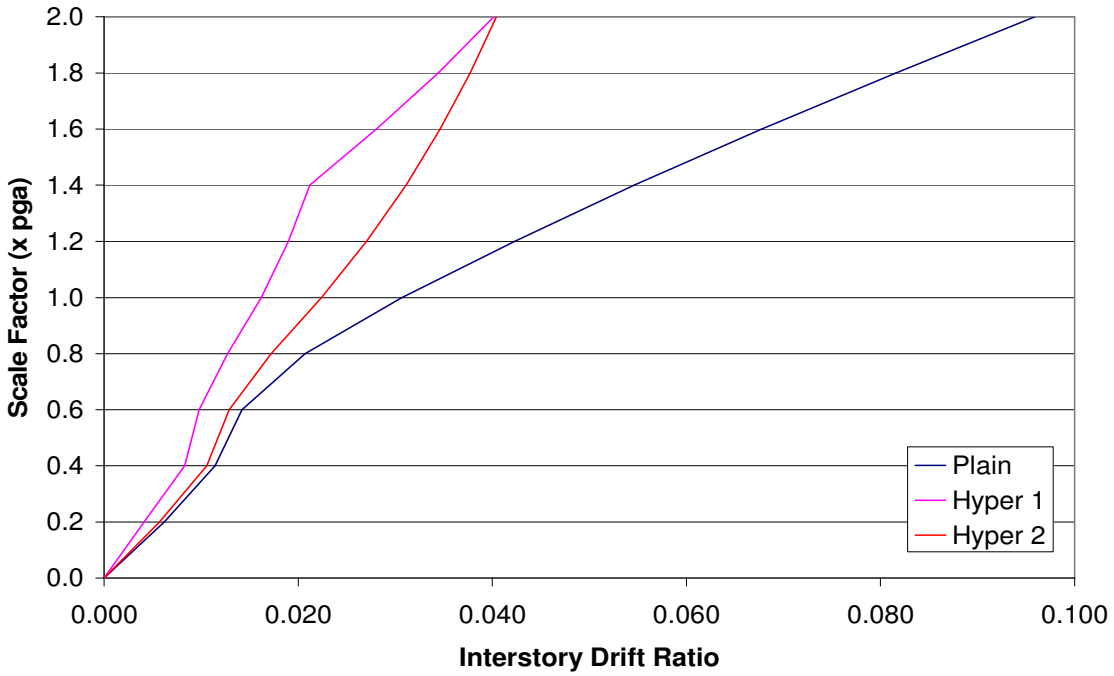

Figure 5.19 – Interstory Drift IDA Curve Summary for P-Delta Case 2, Northridge (Sixth Story)

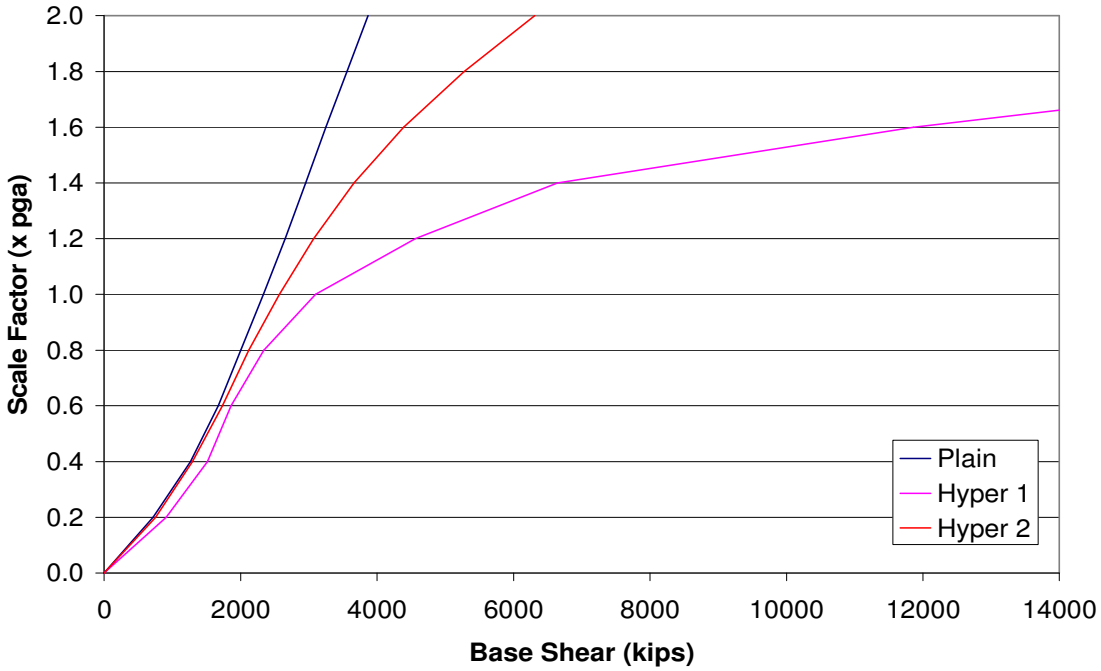

Figure 5.20 - Base Shear IDA Curves for P-Delta Case 2, Northridge

5.5 - Summary of Analyses

A complete set of incremental dynamic analyses was performed on each structural scenario for the moment resisting frame for the investigation of the behavior of hyperelastic braces. Varying the ground motion and P-Delta effects on the system provides a valuable parametric evaluation regarding how the hyperelastic braces influence system response.

The structure was analyzed under the El Centro ground motion for two P-Delta cases. The results are valuable for evaluating the amount of variability present in the system response and the stabilizing effects due to the hyperelastic brace sets. This allows for the braces to be analyzed for their ability to increase system predictability and reduce interstory drift at increasing levels of far-field ground.

An unstable system response was able to be created under the Northridge ground motion so that the hyperelastic braces could be evaluated for their stabilizing potential. Both P-Delta scenarios created unstable system responses, which give valuable insight to the effectiveness of the braces to reduce structural displacements. Most importantly, the

stabilization can also be compared to the related increase in system force to determine the efficiency of the braces.

The IDA curves for maximum system displacement have been created, and they display the same trends shown by the IDA curves for interstory drift. Although the interstory drift IDA curves are summarized for the Northridge ground motion, the IDA curves for the interstory drift of each level have been created. These display the same trends for increased predictability in the IDA curves due to the hyperelastic bracing. These figures may be found in Appendix D.

Overall, the models analyzed under the varying scenarios using IDA create a well rounded view of the performance of hyperelastic braces in MDOF structures. The influence of the braces on system forces at service-level loads is evaluated, and the stabilizing effects are shown through the Northridge ground motion. Both the stable system response as well as the unstable system response provides valuable information on how hyperelastic bracing can remediate undesired structural behaviors.

Chapter 6 – Conclusions and Recommendations

6.1 – Analytical Program Conclusions

Due to the lack of experience with OpenSees as a primary analytical tool for nonlinear dynamic analysis of MDOF structures, many conclusions are reached through the process of gaining expertise with the software. New analytical tools require verification before they can be confidently applied for more advanced purposes. Many rounds of verification and initial analysis were required before the software could be applied to the main analytical focus of the research.

OpenSees is a fully capable and powerful analysis tool that requires more developmental attention before it can reach its full potential. The open source nature of the OpenSees program code has created a new paradigm for structural analysis in which the capabilities of the software are essentially unlimited. The current capabilities of OpenSees have proven to be both adequate and capable for use in the nonlinear dynamic analysis of structures with hyperelastic devices.

Before any future application of OpenSees is recommended on a wide scale, more user support is desired so that assistance is available for those attempting to make new applications with the software. The current support and user's manual provides only a brief insight on the use and application of OpenSees for dynamic modeling.

User interfaces for preprocessing of analytical models and for postprocessing of data are highly recommended. The amount of data that can be produced by OpenSees requires large amounts of processing before any meaning can be ascertained. Handling such large amounts of data through text files greatly enhances the risk of error when processed by hand and contributes to a lack of ease in overall program use.

As more capable user interfaces are created and the learning process for the software is refined, more users will be introduced to the analytical potential of OpenSees. Future applications for the program include use in pseudodynamic testing, nonlinear dynamic analysis, soil-structure interaction, and parametric evaluation of complex systems. The learning curve may be steep for new users, but the capabilities of OpenSees will be greatly enhanced with more developmental attention.

The verification performed on OpenSees shows that the nonlinear dynamic behavior of structures is accurately given by OpenSees. Important modeling benchmarks were established for creating the desired nonlinear dynamic behavior in OpenSees. The verification of the hyperelastic material behavior in OpenSees confirms that the newly programmed materials are accurate for the desired properties. The modeling of nonlinear structural yielding along with hyperelastic material behavior can thus be performed together with the same accuracy. This is verified through the force equilibrium achieved from a combined analysis. With these new and recently established material behaviors, the analysis of the MDOF moment resisting frame with hyperelastic bracing is made possible.

6.2 - Baseline Dynamic Analysis Conclusions

The nonlinear dynamic analysis of the 6-story moment resisting frame provides insight to the behavior of the frame and the influence of the hyperelastic braces. The dynamic analyses under the first P-Delta case demonstrate the behavior of the hyperelastic devices in a stable system. The behavior shows the ability of the hyperelastic device to reduce residual displacements and peak drift values, as well as the tendency for the brace to create over-stiffening responses due to strong pulses in the ground motion.

The over-stiffening response of hyperelastic devices occurs due to a strong pulse in the ground motion acting on a system. The sudden initial displacement, followed quickly by a load reversal as is common in ground motions, can cause the brace stiffness to amplify the deflection under the load reversal. This response primarily occurs when the stiffening response of the hyperelastic brace is responsive to non-yielding levels of displacement in the structure, and thus is more stiff than the system requires for beneficial hyperelastic behavior. The over stiffening effects created by the analyzed sets of hyperelastic braces do not create increased peak drift values; however, they may account for an increase in the base shear response.

Although system forces may increase sporadically, the safety of the system will be increased due to lower potential for dynamic instability. The peak demands of the system remain mostly unaffected, and this explains why the effects are not seen in the

IDA curves. This type of response emphasizes the need for the creation of hyperelastic devices that are effective over the correct range of displacements for a system's behavior.

The influences of the hyperelastic braces in the second P-Delta case are proven to limit the residual displacement and the peak interstory drift response in the system. Both ground motion analyses show improved drift performance of the moment frame with hyperelastic braces. The efficiency of the braces is analyzed through a comparison of the drift and base shear responses.

The increases in base shear are minimal before yielding occurs. The increases in base shear occur at the peak displacement portions of system response, and are related to a beneficial reduction in peak interstory drift. This shows that hyperelastic braces can reduce residual displacement without contributing a detrimental amount of system forces under non-yielding loads.

The reduction of residual displacement by the hyperelastic braces proves their ability to reduce dispersion. Dispersion is decreased as residual displacement is decreased, as shown by the research performed by Oesterle (Oesterle, 2002). The braces can be expected to reduce the amount of dispersion present in a system subjected to incremental dynamic analysis under a wide range of ground motions.

6.3 – Incremental Dynamic Analysis Conclusions

The results of the incremental dynamic analysis of the moment frame provide insight on the performance of the hyperelastic braces in a way that may not be accomplished by a single dynamic analysis. These analyses of the frame allow for the determination of the influence of hyperelastic braces on stable and unstable system responses for scaled increments of ground motion. The analyses give insight on the stabilizing potential of hyperelastic braces and their potential to reduce dispersion through increased response predictability.

The interstory drift IDA curves created under the El Centro ground motion shows that both sets of hyperelastic braces increase the predictability of the structure by lessening the variability in the IDA curves for interstory drift ratios. Along with the limitation of residual displacement shown from the baseline dynamic analyses of the

moment frame, the increased predictability of the system shows that hyperelastic braces can reduce the amount of dispersion present in the behavior of a system.

The results from the IDAs performed under the Northridge earthquake also show the ability of the braces to increase predictability. The graphs of the interstory drift IDA curves become less variant and more predictable as the hyperelastic braces are installed. The frame under the Northridge ground motion responds best to the Hyper 2 braces because the ductility demand of the system under this ground motion matches the ductility range of the Hyper 2 braces the closest.

The stabilizing effects of the hyperelastic braces are shown in the IDA of the moment frame under the Northridge ground motion. The plain frame acquires large amounts of interstory drift to the point where instability is expected to occur. Both sets of braces stabilize the system by limiting the displacement. The braces are also shown to increase system forces only in the higher range of displacement where displacement becomes a concern to the stability of the frame. Together, these show that the desired behavior of the hyperelastic braces is instilled into the moment resisting frame.

Overall, the IDA curves created for the base shears under both ground motions show that the hyperelastic bracing does not contribute a detrimental amount of system forces under non-yielding loads. The base shear may increase at times due to stiffening response such as under the Northridge ground motion, but the main increase in system forces from hyperelastic braces occurs to counteract unstable behavior. Also, the increases in system forces under design level earthquakes may be minimized by choosing the appropriate hyperelastic functions as shown by the Hyper 2 equations under Northridge. These braces were shown to reduce drift while contributing very little to additional base shear in the system.

6.4 – Hyperelastic Brace Effectiveness

The effectiveness of the two types of hyperelastic elements may be determined from the incremental dynamic analyses. The Hyper 1 braces are most influential on stable systems where ductility ranges are smaller and instability is not a problem. A more stable system, as encountered in the IDA of the frame under the El Centro ground motion, is less likely to get far beyond the yield point of the system. This requires the

hyperelastic braces to be more responsive at lower displacements, and the Hyper 1 brace equations provide that level of response. The Hyper 1 brace is most effective under this scenario at reducing peak drift values and at decreasing the variability of the IDA curves. However, since hyperelastic devices are designed mainly as stabilization devices, there will be an increase in system forces for the brace to limit peak displacements in a stable system. For a stable system, linear stiffening devices may provide a more effective means of controlling peak displacements due to the unavoidable increase in system forces introduced by both device types.

The Hyper 2 braces provide hyperelastic behavior that is shown to be most effective over a larger range of displacement. As a result, they are proven to be the most effective braces in controlling the behavior of unstable systems without providing too much stiffness. This effectiveness stems from the fact that an unstable system experiences behavior well beyond the yield strength of the system, and the prescribed hyperelastic brace polynomials can counteract this behavior while limiting their influence at lower demands. This requires a larger range of ductility to be present in the formation of the hyperelastic brace properties, and the Hyper 2 braces match this demand for the moment resisting frame. This is proven in the IDA curves formed under the Northridge ground motion.

The distinctions regarding the effective system types are important for future determination of hyperelastic brace relationships. Although all of the incremental dynamic analyses were focused on achieving instability in the system, the El Centro analyses prove that hyperelastic elements can provide beneficial behavior to a stable system as well. These results provide insight on which hyperelastic brace types should be designated based on the expected range of system behavior.

In forming the polynomial relationships for the hyperelastic braces used in the analysis of the moment frame, the use of the nonlinear system pushover curve is the approved means of gaining the required system parameters. The analyses show, however, that the behavior of the system under a nonlinear pushover analysis is different in many ways than the behavior under a nonlinear dynamic analysis. The pushover analysis shows that the braces are activated over the same range of displacement in the system, and they all gain stiffness at nearly the same point in the structure to produce a collective effect on the system. In a dynamic analysis, the ground motion variances along

with the reaction frequency of the structure cause the system to respond differently than under a pushover analysis. This causes the braces to become activated at differing points from each other, and thus not provide the neat behavior indicated by the pushover analysis.

While the behavior is not altogether different between the analysis types, the formation of the brace equations would benefit in efficiency from an interstory drift analysis under a range of representative ground motions. This would give a better picture of the expected interstory drift values and ductility demand under which the brace equations should be designed, and would result in more efficient and effective hyperelastic brace behavior.

6.5 – Recommendations

Based on the conclusions from the research performed on the moment frame with hyperelastic braces installed, recommendations can be made for continuing research. While the analyses performed on the frame provide some insight into the behavior of hyperelastic devices, further research may be warranted to gain a more complete understanding of their potential.

For future nonlinear analysis, an investigation of structures with hyperelastic devices under a wide variety of ground motions is recommended. This would provide a broad view of the effectiveness of hyperelastic braces under a variety of ground motion characteristics. Multiple ground motions would also allow for the quantification of the reduction in dispersion in the system responses that hyperelastic elements account for.

The quantification of the stabilizing effects of hyperelastic braces may also be desirable for future analysis. The current research shows the limitations that hyperelastic braces provide for system displacements, but a statistically robust representation of the amount of stabilization provided by the braces is outside of the scope of this research. The investigation of structures under a wide variety of ground motions would provide a good basis for quantifying the stabilization provided by the braces. Also, an investigation of the use of hyperelastic elements along with energy dissipation devices may provide insight to further benefits and potential applications.

An investigation of the behavior of hyperelastic braces in systems that exhibit material properties with degrading strength and stiffness is recommended to further assess the effectiveness of hyperelastic bracing. Degrading strength and stiffness in the materials of a structure provide more nonlinearity for the hyperelastic braces to counteract in providing stability. Also, systems with this behavior exhibit more unpredictable behavior, so the analyses would provide another insight regarding the ability of hyperelastic braces to decrease dispersion.

Further quantification of the influence of hyperelastic braces may be performed through the use of more damage indices. More measures of structural behavior would provide a detailed and more extensive insight on how hyperelastic devices control structural behavior, and to what extent each damage measure is influenced. More damage indices would aid in the application of hyperelastic devices for specific damage type remediation.

From a practicality standpoint, the testing of some realistic concepts is recommended to evaluate the feasibility of achieving hyperelastic behavior in a brace design. This would provide a starting point for any laboratory testing focused on evaluating hyperelastic behavior.

The first realistic brace design consists of a set of looped cable elements strung together along a set of fixed nodes as depicted in Figure 6.1. The first set of cables in the element would be looped through with the least amount of slackness, and would gain stiffness first as the element deforms in tension. Each successive set of cables would be looped through the first cable set with increasing amounts of slackness. As the element deforms, each successive set of looped cable elements gains stiffness according to the amount of slackness it originally receives. Since this is a cable element, a cross-bracing design would need to be implemented to gain hyperelastic behavior in both directions of displacement.

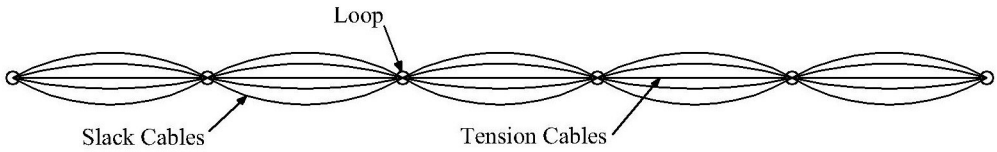

Figure 6.1 – Looped Cable Element for Hyperelastic Bracing

Another brace design involves a set of cable cross-braces linked at the center by a round elastic element as shown in Figure 6.2. As the cables gain tension, the elastic element at the center would deform according to the cable tension. The equations of circular element displacement dictate that the lengthening of the circle in tension would be greater than the corresponding shortening, thus keeping the cable elements in constant tension. The circular elastic element would continue to gain resistance as the cable setup provides increasing displacement. This setup could theoretically provide hyperelastic behavior in a system, as well.

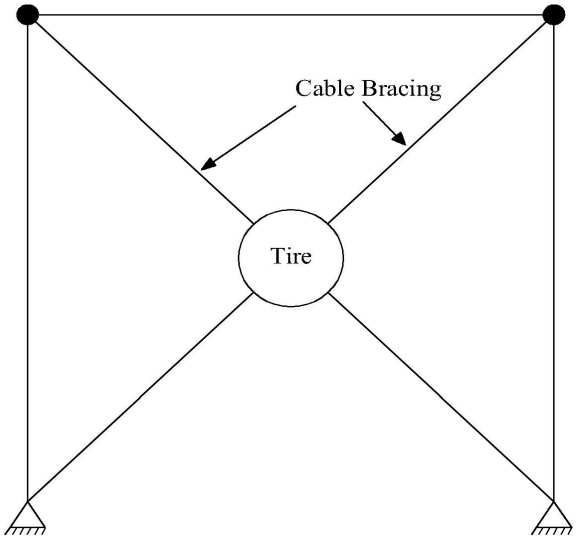

Figure 6.2 – Tire Brace Design for Hyperelastic Behavior

A few preliminary analyses created in OpenSees to model this bracing scheme show similar results to the hyperelastic results found in the original report on hyperelastic elements for SDOF structures (Jin, 2003). The results are promising in indicating the

potential for hyperelastic behavior for this bracing scheme; however, a comprehensive set of analyses has not been performed to evaluate all of the important response parameters for hyperelastic behavior.

The practicality of the second brace recommendation comes in the availability of a round circular element. The use of automobile tires could be theoretically applied in this scenario, depending on the range of elastic behavior demanded by the system. The elastic properties of automobile tires under this type of deformation would need to be investigated to determine the feasibility of this brace design.